Scilight

Nano-electrochemistry & Nano-photochemistry

https://www.sciltp.com/journals/nenp

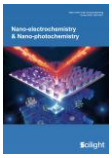

Review

Recent Progress in Hybrid Microalgae-Electrocatalytic/ Photocatalytic Technologies for Enhanced Wastewater Treatment

Sili Qing [1] and Xiaoge Wu [2,*]

[1] State Key Laboratory of Analytical Chemistry for Life Science, School of Chemistry and Chemical Engineering, Nanjing University, Nanjing 210023, China

[2] Environment Science and Engineering College, Yangzhou University, Yangzhou 225009, China

* Correspondence: xgwu@yzu.edu.cn

How To Cite: Qing, S.; Wu, X. Recent Progress in Hybrid Microalgae-Electrocatalytic/Photocatalytic Technologies for Enhanced Wastewater Treatment. *Nano-electrochemistry & Nano-photochemistry* **2025**, *1*(1), 4. https://doi.org/10.53941/nenp.2025.100004.

Received: 28 September 2025
Revised: 2 November 2025
Accepted: 4 November 2025
Published: 13 November 2025

Abstract: Environmental pollution and the freshwater crisis are driving the need for innovative wastewater treatment solutions. Microalgal bioremediation has emerged as a sustainable technology for simultaneous contaminant removal (e.g., COD, nutrients, heavy metals) and biomass production. However, emerging contaminants, refractory pollutants, and complex wastewater matrices often inhibit microalgal growth and degradation efficiency. To address these challenges, this review systematically analyzes three hybrid integration strategies: (i) microalgal microbial fuel cells (MMFCs), (ii) microalgae-electrochemical advanced oxidation processes (EAOPs), and (iii) microalgae-photocatalytic systems. While existing literature extensively covers microalgal biotechnology, comprehensive analyses of its synergistic coupling with nanomaterial-based AOPs (electrochemical/photocatalytic) remain limited. This study elucidates the mechanisms, benchmarking performance, and novel enhancement strategies of these integrated systems, facilitating direct technology comparison. We highlight the multifunctional roles of microalgae in these hybrid systems, including bioelectricity generation (MMFCs), *in situ* oxygen supply (MMFCs and photocatalysis), and biodegradation to mitigate radical quenching (photocatalysis and EAOPs). The comparative advantages and limitations of each technology are critically evaluated, followed by forward-looking perspectives on system scalability, cost-efficiency, and real-world applicability.

Keywords: microalgal microbial fuel cells; hybrid strategy; advanced oxidation processes; electrochemical advanced oxidation processes; photocatalysis; wastewater treatment

1. Introduction

Currently, over 80% of global energy consumption still relies on non-renewable fossil fuels such as coal, oil, and natural gas, leading to significant greenhouse gas emissions that contribute to global warming [1]. This underscores the urgent need to transition to alternative energy sources. Meanwhile, population growth, industrial expansion, and the widespread use of chemicals have led to severe water pollution. The presence of emerging contaminants (ECs) such as endocrine-disrupting chemicals, pesticides, and pharmaceuticals and personal care products in aquatic systems is a serious concern in many countries, posing significant threats to both ecological systems and human health [2]. Additionally, global wastewater generation is estimated at 359.4 billion m^3 per year, with only 188 billion m^3 per year being treated [3]. Reports indicate that the chemical energy contained in industrial wastewater is more than nine times the amount of energy consumed in wastewater treatment [4]. Wastewater generated from various sources is an abundant source of nutrients, and its recovery could help meet the demands

of the growing population. Therefore, there is a critical need to advance efficient and sustainable technologies for sewage treatment and wastewater resource recycling.

Conventional wastewater treatment plants (WWTPs) that rely on activated sludge have several limitations, including high energy consumption (mainly from mechanical aeration), greenhouse gas (GHG) emissions, excess sludge discharge, and inefficient resource recovery [5–7]. The WWTPs often fail to remove multiple antibiotics due to the antimicrobial nature of activated sludge and may even favor the generation and transmission of antibiotic resistance genes (ARGs) [8,9]. Meanwhile, chemical treatment methods raise environmental concerns, while physical methods such as drip filter, membrane filter, and reverse osmosis are limited in their ability to fully eliminate pollutants [10]. These limitations highlight the urgent need for developing energy-efficient, cost-effective, and environmentally sustainable alternatives in wastewater treatment.

In this context, microalgae, as photosynthetic microorganisms, play a significant role in wastewater treatment through mechanisms such as biosorption, bioaccumulation, and biodegradation [11,12]. They efficiently assimilate carbon, nitrogen, and phosphorus from wastewater for biomass synthesis (e.g., proteins, lipids, carbohydrates, and pigments like carotenoids) [13], simultaneously contributing to pollutant removal. Microalgae, which can be prokaryotic or eukaryotic, are widely distributed in marine and freshwater environments and are broadly classified into *Chlorophyta*, *Cyanophyta*, *Chrysophyta*, and *Pyrrophyta* [14]. Carbon accounts for approximately 50% of their biomass by weight, making microalgae a promising source of third-generation biofuels. Their notable attributes include high biomass productivity per unit area, elevated photosynthetic efficiency (4–8%, surpassing that of non-aquatic plants) [15], rapid growth, and substantial CO_2 sequestration capacity—with one ton of microalgae consuming about 1.83 tons of CO_2, accounting for nearly one-third of global CO_2 fixation [16], Microalgae also produce valuable compounds such as proteins, ω-3 fatty acids, and pigments [17] and exhibit tolerance to a wide variety of environmental conditions [18]. These characteristics, combined with their ability to remove pollutants and mitigate greenhouse gases, make microalgae a sustainable and multifunctional technology for modern wastewater treatment plants. However, the photosynthetic efficiency and growth of microalgae are often limited in recalcitrant wastewaters, such as anaerobic digesters, industrial effluents, and antibiotic-containing wastewaters, due to high pollutant concentrations, toxicity, or chromaticity.

To achieve efficient pollutant removal, integrated systems combining microalgae with microalgal microbial fuel cells (MMFCs) and advanced oxidation processes (AOPs) have gained increasing attention [19,20]. MMFCs are an advanced form of traditional microbial fuel cells (MFCs), in which microalgae are applied in the cathodic chamber to supply O_2 (as the electron acceptor) and replace mechanical aeration [21–23]. MMFCs enable the generation of bioelectricity in wastewater and the removal of pollutants, offering good biocompatibility, lower energy consumption, and continuous operation [24–26]. On the other hand, AOPs, including electrochemical advanced oxidation processes (EAOPs) [27,28] (e.g., electro-Fenton, EF) [29,30] and photocatalysis [31,32], generate highly reactive oxygen species (ROS), primarily hydroxyl radicals (•OH), to effectively eliminate persistent organic pollutants. Hydroxyl radicals have a very high standard potential ($E_{[\bullet OH/H2O]}$ = 2.80 V vs. SHE) that enables them to non-selectively react with a variety of contaminants, converting them into hydroxylated or dehydrogenated products, and ultimately to CO_2, H_2O, and inorganic ions [33]. However, standalone AOPs often require extended reaction times to achieve complete mineralization, leading to high operational costs [34]. To enhance economic feasibility, a common strategy involves using AOPs as a pretreatment step to improve wastewater biodegradability within short residence times, followed by microalgae-based biological treatment for further degradation of residual contaminants, including chemical oxygen demand (COD), nitrogen, and phosphorus [11,35]. This combination leverages the complementary strengths of each process: AOPs rapidly decompose recalcitrant molecules, while microalgae contribute to nutrient removal and resource recovery, offering a synergistic and sustainable approach for treating refractory wastewaters [36,37]. In microalgae/EAOPs systems, a sequential treatment strategy is often adopted: an electrochemical pre-treatment step enhances wastewater biodegradability, while subsequent microalgae treatment thoroughly removes residual COD, nitrogen, and phosphorus [38–40]. Meanwhile, the microalgae/photocatalytic technology utilizes light energy without additional energy input, resulting in very low operational energy consumption [41,42].

Critical overviews of microalgae-coupled AOPs used to date have been limited. The present review aims to provide a comprehensive summary of the recent progress of MMFCs and microalgae-coupled AOPs (EAOPs and photocatalysis) for wastewater treatment (Figure 1). It outlines the fundamental metabolic pathways of microalgal bioremediation and the key conditions influencing microalgal growth. Furthermore, the advantages and disadvantages of each hybrid technology are critically discussed, with a particular focus on the removal efficiency and the potential mechanisms. Finally, current challenges in this area and further research perspectives are also addressed.

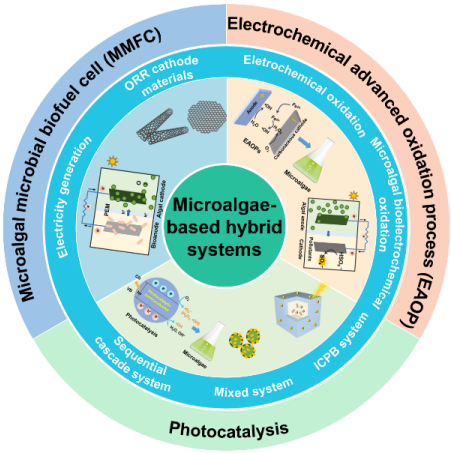

Figure 1. The scheme of microalgae-based hybrid systems. PMS, peroxymonosulfate; ICPB, intimately coupled photocatalysis and biodegradation.

2. Bioremediation by Microalgae: Metabolic Pathways and Growth Condition Optimization

Microalgae offer a promising alternative in wastewater treatment by effectively consuming organic matter and inorganic components (including nitrogen, phosphorus, and some metals) in wastewater. This process not only removes pollutants but also generates valuable biomass for bioenergy and commercial products in an environmentally friendly manner. Numerous microalgal species, including *Chlorella, Scenedesmus*, *Phormidium*, *Dictyosphaerium* sp., *Chlamydomonas*, *Botryococcus,* and *Limnospira* (formerly *Arthrospira, Spirulina*) have been widely recognized for their efficient wastewater bioremediation capabilities [43,44]. Microalgae metabolize the nutrients and organic matter available in wastewater through heterotrophic or mixotrophic metabolism. Microalgae are autotrophic (require only inorganic compounds such as carbon dioxide (CO_2) and salts) and heterotrophic (require an organic source) in nature. The metabolic process is shown in Figure 2. The mechanisms of microalgal bioremediation systems for removing contaminants mainly include bioadsorption, bioaccumulation, and biodegradation [45]. During the photosynthetic activity, microalgae have an immense capacity for CO_2 fixation and O_2 release through photosynthesis, thereby contributing to climate change mitigation without generating secondary pollution. Microalgae can also consume other soluble carbonate forms (CO_3^{2-}, HCO_3^-) either directly or after converting them into CO_2 by carbonic anhydrases [46,47]. Nitrogen (N) and phosphorus (P) are two major water pollutants in water bodies that can cause eutrophication, water blooms, and red tides [48]. Microalgae can assimilate N and P into cellular constituents such as amino acids, proteins, carbohydrates, nucleic acids, lipids, and other value-added products via absorption and metabolic incorporation. Inorganic nitrogen in wastewater has different forms, such as nitrite (NO_2^-), nitrate (NO_3^-), and ammonium (NH_4^+), all of which can be taken by microalgae with the help of ammonium and nitrate/nitrite transporter proteins [49]. Inside the cell, NO_3^- and NO_2^- are finally reduced to NH_4^+ by nitrate reductase and nitrite reductase located in the cytosol and chloroplast, respectively [49]. Eventually, NH_4^+ is assimilated into biomass through the glutamine synthetase/glutamate synthase (GS/GOGAT) pathway. The nitrogen assimilation process in microalgae differs from anaerobic ammonium oxidation (anammox), which directly oxidizes ammonium using nitrite as an electron acceptor to produce nitrogen gas, requiring no organic carbon or aeration. Phosphorus, present mainly as organic phosphate or orthophosphates (e.g., $H_2PO_4^-$, HPO_4^{2-}), is assimilated through phosphorylation processes such as oxidative phosphorylation, substrate-level phosphorylation, and photophosphorylation pathways, which generate adenosine triphosphate (ATP) from adenosine diphosphate (ADP) to support cellular metabolism in wastewater [50].

Heavy metals are effectively eliminated by microalgae through a two-stage process: (i) a rapid and non-metabolic extracellular adsorption onto the cell wall (polysaccharides, lipids, carbohydrates, and proteins); (ii) a slow metabolism-dependent intracellular uptake and accumulation within the cytoplasm [51]. Functional groups such as carboxyl, sulfate, and phosphate groups in the algal cell walls are responsible for uptake (biosorption) of metal ions via mechanisms such as chemisorption, chelation, ion exchange, physical entrapment, complexation, and micro-precipitation [52]. In contrast, the slower metabolic process involves active transport across the cell membrane and internal accumulation within cellular structures [53]. Moreover, some heavy metals serve as essential micronutrients for microalgal growth, such as Zn, Cu, Mn, Ni, and Co, while others (e.g., Cd, Pb, and Hg) exhibit toxicity and have unknown biological functions [54]. Notably, due to the hormesis effect, low concentrations of metals can stimulate microalgal growth, while higher concentrations inhibit it by disrupting metabolic processes [55].

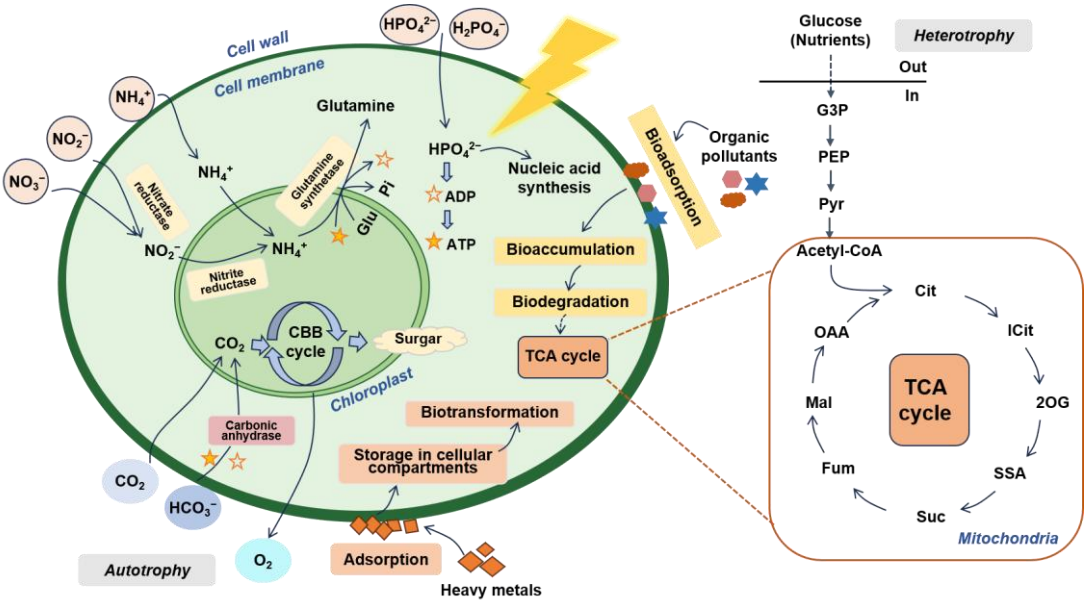

Figure 2. Mechanism based on microalgae for wastewater bioremediation and biomass production, and the carbon metabolism in glycolysis and TCA. CBB cycle, Calvin-Benson-Bassham cycle; Glu, Glutamine; Pi, inorganic phosphate; TCA cycle, tricarboxylic acid cycle. The carbon metabolites: G3P, glyceraldehyde-3-phosphate; PYR, pyruvate; PEP, phosphoenolpyruvate; OAA, oxaloacetate; Mal, malate; Fum, fumarate; SSA, Succinyl semialdehyde; Suc, succinate; 2OG, 2-oxoglutarate; Cit, citrate; iCit: isocitrate; G3P, glyceraldehyde 3-phosphate.

Microalgae can be cultivated under four primary trophic modes: autotrophic, heterotrophic, mixotrophic, and photoheterotrophic [56]. In the autotrophic mode, microalgae utilize sunlight and inorganic carbon. The heterotrophic mode relies on organic carbon for both energy and growth, while the mixotrophic mode can simultaneously use both light (with inorganic carbon) and organic carbon. Conversely, the photoheterotrophic mode requires both light for energy and organic carbon for growth, but does not rely on CO_2 as a primary carbon source. The growth of microalgae is influenced by various physical and chemical factors, including light, temperature, nutrient availability, pH, and CO_2 concentrations. (i) Light (intensity, wavelength, and duration of the photoperiod) significantly influences the growth and makeup of microalgae biomass (fatty acid and pigment profiles) [57,58]. Light intensity influences photosynthesis by impacting photosystem II (PSII) activity and the fluidity of the thylakoid membrane. Amongst the monochromatic light, the red and blue lights are most preferred for high-rate algal cultures [59]. Generally, increasing light intensity boosts the growth rate of microalgae, whereas low light intensities may restrict cell growth and increase chlorophyll content. However, excessively high light intensities can lead to photo-inhibition [60]. (ii) pH affects the enzyme activity related to the metabolism of microalgae and the ion absorption efficiency of microalgae, which in turn affects cell growth, carbon fixation efficiency, and all other related biochemical reactions impacted by pH changes. They normally prefer a pH range between 6.5 and 8.5 for growth [61]. (iii) Additionally, temperature plays a significant role in determining the enzymatic activity and significantly influences the photosynthesis process, cellular chemical composition, nutrient uptake, CO_2 absorption, and growth rates across all algal species. While microalgal growth is optimal between 16 and 27 °C, it slows below 16 °C and becomes markedly constrained above 35 °C as metabolic processes are impaired [62]. (iv) Adequate amounts of CO_2 are required for triacylglycerol (TAG) synthesis, while excessive CO_2 leads to the loss of microalgal biomass. 2–5% (*v*/*v*) of CO_2 supplementation to microalgae has been found to enhance biomass productivity [63]. These parameters vary among different microalgae species. (v) In addition to carbon, nitrogen, and phosphorus are known to be the main nutrient sources for supporting microalgal growth, which can be sourced from waste streams [64]. N:P ratio in the culture has a significant impact on the growth of algae and the biochemical composition of the algal biomass [65]. Under a low N:P ratio of 9, microalgae can accumulate a large amount of lipid and carbohydrates while reducing the protein content in the biomass, with lipid levels rising notably under nitrogen starvation [66].

3. Microalgal Microbial Fuel Cell

In MMFCs, microalgae growing in the cathodic compartment eliminate the need for artificial O_2 and enhance overall power density, replacing mechanical aeration (air pumping). It has been reported that energy consumption for aeration accounted for 45–75% of the expenditure of WWTPs in the US [67]. Therefore, the use of microalgae

to supply oxygen significantly reduces both energy demand and operational costs. Besides, MMFCs offer numerous benefits, including producing sustainable electricity, wastewater treatment, CO_2 reduction, and the generation of sustainable bioproducts such as fuels, fertilizers, food items, and pigments [22].

The most common design of MMFCs is the dual-chamber configuration (Figure 3a,b), consisting of an anodic chamber with heterotrophic electrogenic bacteria and a cathodic chamber with microalgae, separated by a proton exchange membrane (PEM). Exoelectrogenic bacteria in the anode chamber (e.g., *Geobacter sulfurreducens*, *Shewanella oneidensis*, *Rhodopseudomonas palustris*) function as the core biocatalysts by oxidizing organic substrates (e.g., acetate) and exocellular electrons (Equation (1)). These electrons are transferred to the anode via direct contact or indirect pathways (nanowires and endogenous mediators). This mechanism allows direct conversion of chemical energy into electricity, while protons migrate to the cathode chamber through the PEM. Meanwhile, in the cathodic chamber, oxygen produced by microalgae via photosynthesis (Equation (2)) serves as the terminal electron acceptor (TEA), undergoing a 4-electron oxygen reduction reaction (ORR, Equation (3)). This process ultimately completes the electron transfer cycle within the system [68].

Anode:

$$C_6H_{12}O_6 + 9H_2O \rightarrow 3CO_2 + 3HCO_3^- + 27H^+ + 24e^- \quad (1)$$

Cathode:

$$nCO_2 + nH_2O \rightarrow (CH_2O)n + nO_2 \quad (2)$$

$$O_2 + 4H^+ + 4e^- \rightarrow 2H_2O \quad (3)$$

In traditional MFCs, oxygen is supplied to the cathode either via passive or active aeration by means of mechanical aerators. The photosynthetic oxygenation in the cathode of MMFCs can be achieved in two ways. Algae can grow in the cathode chamber itself to *in situ* generate and utilize O_2 (Figure 3a). Alternatively, algae can grow in separate glass bottles (termed as photobioreactor; PBR) connected to the cathodic chamber of MFCs, where the produced O_2 can be supplied through silicon pipes to the cathode (Figure 3b) [69]. Multiple studies have demonstrated that photosynthetic oxygen supply by microalgae yields superior electricity production compared to mechanical aeration [70,71]. Ramesh Kakarla et al. [72] applied *Scenedesmus obliquus* to the MFC cathode, the dissolved oxygen (DO) concentration under photosynthetic aeration reached 15.7 mg L^{-1} in a sealed reactor (a supersaturation condition), and the power output reached 153 mW m^{-2}, representing a 32% increase compared to the maximum power density (116 mW m^{-2}) under mechanical aeration (DO = 5.9 mg L^{-1}).

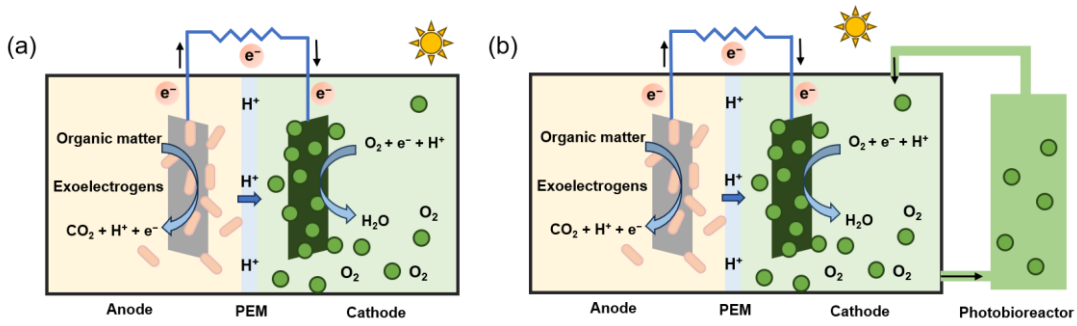

Figure 3. (**a**) Schematic of MMFCs with a dual chamber. (**b**) Dual-chamber MMFCs with a photobioreactor.

Research is underway to improve ORR kinetics to enhance the electricity production of MMFCs. ORR at the cathode is highly dependent on the DO concentration in the catholyte. Microalgae species and operational conditions (such as light intensity, light/dark cycles, pH, and CO_2) significantly affect DO production [73]. It has been reported that at least 2.2 mg L^{-1} concentration of DO should be maintained in the cathodic chamber to achieve a higher amount of coulombic yield [74]. However, ORR performance was not proportionally increased with the increase of DO, possibly due to the limitations in the ORR kinetics and mass transport of oxygen at the cathode [75]. To address the challenges of low power generation and bioenergy recovery efficiency of MMFCs, Liang et al. [73] systematically investigated the effect of cathode operational parameters on system performance. Their study involved screening microalgae species, optimizing light intensity (1400, 2100, and 3200 lux), and adjusting light/dark cycle durations (12 h/12 h, 18 h/6 h, and 24 h/0 h). Results demonstrated that *C. vulgaris* under 3200 lux with an 18 h/6 h cycle achieved the highest power output (126 mW m^{-3}) and electrochemical activity. *C. vulgaris* achieved the highest power output, followed by *Chlorella* sp., *Tetradesmus obliquus*, and *Microcystis*

aeruginosa. This was attributed to its significantly higher DO concentrations. The higher DO concentration not only enhanced O_2 availability for ORR but also facilitated greater electron transfer, thereby boosting both the output voltage and overall power density.

3.1. ORR Cathode Materials in Microalgal Microbial Fuel Cells

In addition to increasing oxygen concentration, the cathode material has a major effect on the power generation capacity of MMFCs by influencing the efficiency of electron transport and ORR activity [76]. The ORR performances of cathode materials are usually limited during practical operation conditions by activation energy barrier, ohmic overpotentials, and mass transport resistance [77]. The development and study of ORR catalysts to lower the energy barrier of intermediates, weaken the O–O bond of O_2, and facilitate the evolution of the reaction toward a $4e^-$ ORR pathway is crucial. Common ORR catalysts include carbon and doped carbon materials, noble metals, transition metal materials, and biomass materials.

Metal-based catalysts (including noble metal materials, transition metal materials, and their derivatives) are highly effective for ORR due to the strong interaction between the vacant *d*-orbitals of the metal centers and oxygen molecules, which can facilitate the breaking of the O–O bond [78]. Noble metals, characterized by abundant empty orbitals and confined electrons, exhibit high electron mobility and conductivity. Commonly used noble metal catalysts in MFC cathodes include platinum (Pt), palladium (Pd), and gold (Au) [79]. Pt particularly facilitates ORR by significantly reducing the activation overpotential of ORR. It remains the most efficient and widely used catalyst in both MFCs and MMFCs [80]. However, the practical application of Pt cathode materials is limited by their high cost, constrained availability, and relatively low durability [81]. Therefore, reducing the use of Pt by preparing Pt complexes with other materials (e.g., alloying modifications) or developing novel catalysts to replace Pt is a more feasible and economical approach [82,83]. Transition metals such as Mn, Fe, Cu, Co, and Ni are mostly applied because they can illustrate excellent physicochemical properties and high activities in the ORR process [84,85]. This could be due to their unique spinel structures and presence of variable oxidation states. Moreover, they are also non-toxic and environmentally friendly [77]. Yang et al. [86] prepared a series of Co-based ternary metallic metal–organic frameworks (CN/CNTs/$Zn_3Co_2Fe_{0.1}$-S-900) with controllable metal ratios as an efficient ORR catalyst through a facile sulfuration-pyrolysis treatment. The proposed catalyst achieved comparable ORR activity and superior durability to the Pt/C, due to the formation of a three-dimensional porous structure that facilitated electron transport. The maximum power density of MMFC (850 mW m^{-2}) indicated a rise of 59.5% by this sample, compared with the level of Pt/C (533 mW m^{-2}). On the other hand, a few non-noble metal-based catalysts, like the stainless steel mesh [87] and nickel foam (NF) [88], have also been used in biocathodes in MMFCs. In spite of having high electrical conductivity, these materials possess less surface area, less resilience towards corrosion, and in some cases, toxicity towards algal strains [89]. As a result, they have usually been selected as support materials to load catalysts and microorganisms.

Development of low-cost nanoparticle-based biocompatible cathode materials has become a primary research focus for enhancing ORR performance in algae-assisted cathodes. Carbon materials, including biochar [90], carbon felt [91,92], graphite felt [93], carbon cloth [94], and carbon fiber brush [71], have garnered significant attention due to their high stability, abundance of raw materials, and cost-effectiveness. However, these materials typically exhibit limited active sites and low ORR catalytic efficiency. With the rapid advancement of nanotechnology, low-dimensional carbon nanomaterials such as carbon nanotubes (CNTs), graphene, and graphene derivatives have demonstrated superior ORR catalytic activity in MFCs [95–97]. Nevertheless, these carbon-based materials predominantly follow a $2e^-$ ORR pathway, leading to energy dissipation and the generation of H_2O_2 as a byproduct, which poses toxicity risks to microalgae [98].

It is well-established that heteroatom doping is an effective strategy for developing efficient and durable carbon-based cathode catalysts with enhanced $4e^-$ ORR activity. Heteroatom-doped carbon materials exhibit high conductivity, adjustable structure, high catalytic efficiency, and high corrosion resistance. Heteroatoms generally include B, O, F, N, S, and P [99]. The functionalization of carbon layers by nitrogen doping increases the surface polarity of carbon materials and introduces extrinsic defects, enhancing electronic conductivity and ionic mobility [100]. Qin et al. [101] coated gadolinium-cobalt (Gd-Co) nanosheet arrays onto nitrogen-doped carbon spheres (N-CSs) supported by nickel foam (NF), creating a unique three-dimensional hierarchical-structured Gd-Co@N-CSs/NF cathode material. The high electrochemical catalytic activity (Gd sites) and large specific surface area (3D hierarchical structure) improved ORR catalytic kinetics and electron transfer while shortening charge transfer and electrolyte diffusion pathways. Compared to control groups, its 3D hierarchical structure enabled a higher loading capacity for algal cells. If N-doped carbon is combined with transition metals (M) to form metal-nitrogen-carbon (M-N-C) catalysts, the number of active sites and the conductivity of carbon materials can be improved further

[79]. The coordination of metal and nitrogen in the matrix effectively regulates the local electronic structure, improves the distribution of local charge density, produces more active sites, and thus enhances catalytic activity. Thereby, the strong interaction between M-N-C components promotes the $4e^-$ ORR process by activating the O−O bond [102]. A Fe-N-C nanocomposite catalyst was successfully synthesized by pyrolyzing pomelo peel, $FeCl_3 \cdot 6H_2O$, and melamine [103]. The results showed that graphitized structures, pyridine-N, and graphitic-N enhanced the conductivity of biomass-derived carbon. The MFC with the Fe-N-C-based cathode delivered a maximum power density of 184 $mW \cdot m^{-2}$, outperforming a Pt/C reference catalyst (134 $mW \cdot m^{-2}$). While M-N-C catalysts have already been employed as cathode materials in MFCs, their application in algae cathodes is still under development. Table 1 summarizes the performance of metal-based ORR catalysts.

Table 1. Metal-based ORR catalysts and their performance and cost.

Configuration	Microorganisms	Anode	ORR Cathode Catalysts	Cost of Cathodes	Power Density ($mW\ m^{-2}$)	COD Removal	Refs.
MFC	Inoculated with wastewater	Carbon fiber brush	Nickle foam/activated carbon	\$50·m^{-2} Pt/carbon cloth = \$1500 m^{-2}	1190 ± 50 1320 (Pt/carbon cloth)	/	[104]
MFC	Inoculated with wastewater	General carbon particles	Co-doped OMS-2	5% of the platinum cost	180	99.6% 86.7% (Pt)	[105]
			OMS-2	5% of the platinum cost	86 198 (Pt)	66.7 86.7% (Pt)	
MFC	Inoculated with wastewater	CB/PTFE/SSM	FFC/NG@AC-3	1.16 \$·g^{-1} Pt/C = 33 \$·g^{-1}	1913 1454 (Pt/C)	80.2%	[106]
MFC	Inoculated with wastewater	Graphite granules	Spinel Cu–Co oxide ($Cu_{0.30}Co_{0.70}$) Co_2O_4 (on acetylene black)	12 times lower versus Pt-based cathodes	567.58 (87% of Pt-sprayed cathodes)	56% 64% (Pt)	[107]
MFC	Sewer sludge	Carbon rod	Cu/TiO_2 nanoparticles	1/70 that of Pt catalysts	312	/	[108]
MFC	Inoculated with domestic wastewater	Graphite carbon brush	FeCoS(MOF)	0.023 \$·cm^{-2}	861.5 337.9 (Pt/C)	/	[109]
MMFC	Anode: Activated sludge; Cathode: *Chlorella vulgaris*	Carbon felt	Gd-Co@N-CSs/NF	4.3 \$·g^{-1} Pt/C = 33 \$·g^{-1}	115.9	92.1%; COD degradation rate: 57.5 $mg \cdot L^{-1} \cdot h^{-1}$	[101]
MMFC	Anode: Activated anaerobic sludges; *Scenedesmus obliquus* (FACHB13) in a photobioreactor	Not mentioned	CN/CNTs/ $Zn_3Co_2Fe_{0.1}$-S-900	1.8 \$·g^{-1} Pt/C = 42.65 \$·g^{-1}	850 533 (Pt/C)	/	[86]
MFC	*Escherichia coli*, *Pseudomonas aeruginosa*, *and Brevundimonas diminuta*	Graphite felt	*G/C–Fe-2	0.93 \$·g^{-1} Pt/C(20%) = 1116 \$·g^{-1}	560 818 (20%Pt/C)	/	[110]
MFC	Activated sludge	Carbon brush	Iron–mebendazole (Fe-MBZ)-based M–N–C catalysts	3.40–3.60 \$·g^{-1} Pt = 150 \$·g^{-1}	610–680 940–990 (Pt)	/	[111]

Note: FFC/NG@AC-3, Fe/Fe_3C nanospheres (FFC@NG) on activated carbon (AC) (20% mass ratio); Gd-Co@N-CSs/NF, gadolinium-cobalt (Gd-Co) nanosheet arrays onto nitrogen-doped carbon spheres (N-CSs) supported by nickel foam (NF); FeCoS(MOF), MOF-derived oxygen-defect-rich $FexCo_{3-x}S_4/Fe_yCo_{9-y}S_8$; CN/CNTs/$Zn_3Co_2Fe_{0.1}$-S-900, carbon nanopolyhedron (CN)/carbon nanotubes (CNTs)/metal sulfides; OMS-2, manganese oxides with a cryptomelane-type octahedral molecular sieve; *G, gelatin.

Recently, metal-free catalysts, especially those based on biochar, have been utilized as ORR catalysts in MFCs due to their excellent electrical conductivity, low cost, and high specific surface area [112,113]. Derived from plant or animal waste (such as chitosan, pectin, and cornstalk biomass) represents an abundant and inexpensive source of carbon-rich precursors [114–116]. Moreover, biomass naturally contains elements such as C, N, O, and S, enabling the formation of heteroatom-doped carbon materials through direct pyrolysis [117]. Common modification strategies for biochar involve blending or co-synthesis with other carbon materials, as well as doping with metallic elements [118,119]. These biomass-derived catalysts offer a cost-effective alternative for MMFCs, provided they deliver sufficient power output.

3.2. Removal of COD, Nutrients, and Heavy Metals

Owing to the diversity of algal metabolism (mixotrophy), MMFCs are capable of treating nutrient-rich wastewater [56]. Microalgae utilize the carbon contaminants present in wastewater by a heterotrophic or mixotrophic mode of operation. Besides, microalgae uptake nitrogen (in the form of ammonium and nitrate) and phosphorus (as phosphate) by the assimilation pathway [64]. Therefore, microalgae not only enhance the bioelectricity but also remove extra COD and nutrients when the anodic effluent is fed to the cathodic chamber. They recycle these nutrients into microalgae biomass, which can be further converted to biofuels or other valuable co-products. The MMFCs have been used to treat various wastewater, including pharmaceutical wastewater [120,121], domestic wastewater [70,122], landfill leachate [123,124], industrial wastewater [125–127], livestock wastewater [128], and food wastewater [129,130]. The efficiency of MMFCs for carbon removal, nutrient removal, and power production has been improved substantially over the last decade [22,131]. Table 2 presents several representative MMFC systems and summarizes their performance. For example, Yang et al. [132] constructed an MMFC to treat real domestic wastewater, and the system realized higher removal efficiencies of total nitrogen (TN, 96.0%), total phosphorus (TP, 91.5%), and COD (80.2%) than those of the MFC or algae biofilms alone. The highest power density of MMFC (62.93 $mW \cdot m^{-2}$) was 18% higher than that of MFC (52.33 $mW \cdot m^{-2}$), and a lipid productivity of 6.26 $mg \cdot L^{-1} \cdot d^{-1}$ could be obtained simultaneously. Wang et al. [122] developed an MMFC to determine the contribution of microorganisms for pollutant removal. Results showed that organic matters were predominantly removed in the anodic chamber, in which electricity generation, sulfate reduction, fermentation, and methanogenesis might occur. Meanwhile, nutrient assimilation into microalgal biomass in the cathodic chamber accounted for 27.7–50.0% of nitrogen and 37.1–67.9% of phosphorus removal. Notably, the synergistic interactions among photosynthesis, nitrification, aerobic denitrification, and autotrophic denitrification in the cathodic chamber significantly contributed to the high TN removal efficiency [121].

In order to improve the removal efficiency of nutrient ions, Jiang et al. [124] established a self-sustaining photomicrobial nutrients recovery cell (PNRC) (Figure 4a). Instead of directly introducing eutrophic water into the electrode chambers, this system concentrated NO_3^--N and PO_4^{3-}-P in the anode and NH_4^+-N in the cathode via a self-generated electric field, facilitating recovery as microalgal biomass. At an external resistance of 200 Ω, the current density of the PNRC reached 2.0 $A \cdot m^{-2}$, enabling over 92% separation of NH_4^+-N, NO^{3-}-N, and TP from eutrophic water, with subsequent removal efficiencies of 91.8%, 90.6%, and 94.4%, respectively. Moreover, Elmaadawy et al. [123] advanced the system configuration and proposed an algal biofilm MFC equipped with a bioactive oxygen-consuming unit (AB-OCU-MFC) for treating leachate containing refractory organics and high-strength NH_4^+-N (Figure 4b). The COD and NH_4^+-N removals in AB-OCU2-MFC (2 cm thickness of circular carbon felt) increased by 16.72% and 59.1% compared to the standalone MFC and increased by 13.3% and 9% compared to the control algal biofilm reactor. The improvements were attributed to the enhanced anaerobic environment in the anode, coupled with efficient bioactive nitrification and denitrification in the OCU, where exoelectrogenic anode bacteria and denitrifying cathode bacteria were significantly enriched. In addition, the heavy metals widely exist in industrial wastewater, which have an adverse effect on the biological wastewater treatment processes. MMFC has been reported to be a feasible and effective approach for heavy metal removal (95% Cd^{2+}) in the algal-cathode by hydroxide precipitation and biosorption [88]. Yang et al. [133] established an algae-assisted triple-chamber MFC that simultaneously removed Cu^{2+}, COD, and nitrogen while generating electricity (Figure 4c). The Cu^{2+} removal efficiency reached 99.9% after treatment in the first cathodic chamber (86.2%) and assimilation by algae (4.7%).

The type and complexity of substrates significantly influence the efficiency of power generation in MMFCs, as more complex substrates are less biodegradable by anaerobic microorganisms, thereby limiting both electricity generation and COD removal efficiency. To address these limitations, researchers have adopted various operational strategies, including screening and acclimating specific pollutant-degrading bacteria/microalgae [68,134], optimizing hydraulic retention time (HRT) [135], optimizing the mode of substrate supply (batch-fed modes or continuously fed systems) [120,136], as well as promoting electron transfer efficiency and metabolic activity of anodic biofilms. Zhang et al. [120] proposed a continuous-flow Fe^0-catalyzed MMFC, where Fe^0 prevented algal growth in anodes and achieved a 50% improvement in power production performance (Figure 4d). The addition of Fe^0 significantly improved the removal of chlortetracycline by improving the activity of microorganisms in the anode, while reducing the risk of transmission of ARGs and mobile genetic elements (MGEs). The anode-cathode continuous flow operation mode avoided anode acidification and facilitated efficient nutrient uptake in the cathode by microalgae using the treated effluent.

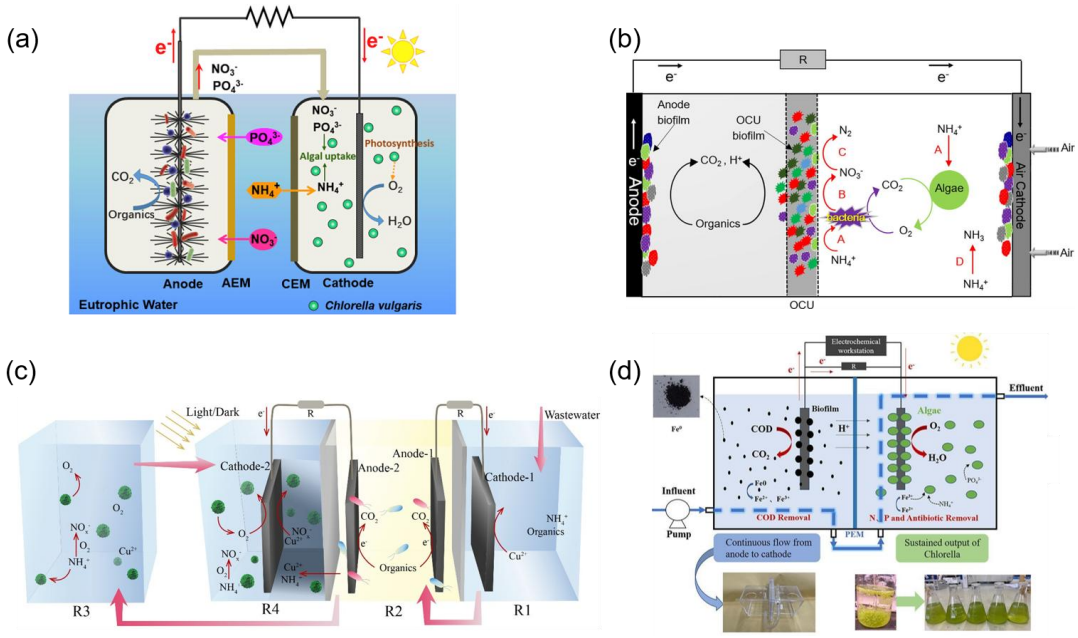

Figure 4. (**a**) Schematic diagram of the PNRC system. AEM: anion exchange membrane; CEM: cation exchange membrane. Reprinted with permission from Ref. [124]. Copyright 2019, copyright Elsevier. (**b**) The coupling effect of algal biofilm with an OCU for organic and nitrogen removal. The OCU placed between the anode and the cathode acted as an oxygen barrier to enhance nitrogen removal. The key processes involved are: (A) assimilation process, (B) nitrification process, (C) denitrification process, and (D) volatilization process. Reprinted with permission from Ref. [123]. Copyright 2020, copyright Elsevier. (**c**) Schematic of the algae-assisted triple-chamber MFC (R1, R2, and R4) and the photobioreactor (R3). The MFC included an anode chamber (R2) and two cathode chambers (R1, R4). An AEM separated R1 and R2 to block Cu^{2+} transfer, while a CEM between R2 and R4 permitted NH_4^+ and Cu^{2+} diffusion. A photobioreactor (R3) pre-treated R2 effluent to enhance ammonium removal before entering R4. Reprinted with permission from Ref. [133]. Copyright 2021, copyright Elsevier. (**d**) Fe^0-catalyzed MMFC in continuous flow operation mode enhanced antibiotic removal. Reprinted with permission from Ref. [120]. Copyright 2023, copyright Elsevier.

Table 2. Configurations, performance, and mechanisms of MMFC systems.

Reactor Construction	Electrodes	Microalgal Species	Tape of Wastewater	Removal Rate (%)	Power Output	Biomass	Mechanisms	Refs.
Dual-chambered MMFC	Anode: graphite felt; Cathode: graphite felt	*Chlamydomonas reinhardtii*	Synthesized wastewater	7 days; COD: 73.30% (0.32 Kg·COD m^{-3} day^{-1})	15.21 $W·m^{-3}$	4.6 $g·L^{-1}$ (0.284 day^{-1})	*C. reinhardtii* supports high power output from an MMFC and is highly resourceful in terms of value-added products.	[68]
Dual-chambered MMFC	Anode: carbon felt; Cathode: carbon felt	*Chlorella* sp.	2% fat, oil, and grease (FOG)	15 days; COD: 100%; TN: ~75%; TP: 76%	21.0 $mW·m^{-2}$	/	Continuous cycling of microalgae enhances the availability of oxygen and the biocatalytic activity of the cathode.	[137]
Dual-chambered MMFC	Anode: carbon felt; Cathode: Gd-Co@N-CSs/NF	*Chlorella vulgaris*	Synthetic wastewater	2 days; COD: 92.1%; COD degradation rate: 57.5 $mg·L^{-1}·h^{-1}$.	115.9 $mW·m^{-2}$	Cell density increases 55.6% after 360 h; 14.5 $mg·g^{-1}$	The unique 3D Gd-Co@N-CSs/NF architecture offers exceptional 360-h stability (5.8% voltage drop), high power density, and enhances microalgae growth.	[101]
Dual-chambered MMFC	Anode: carbon felt; Cathode: Gd-Co@N-CSs/NF	*Chlorella vulgaris*	Synthetic wastewater	50 h; COD: ~98%; NH_4^+-N: 83.84%; TP: ~45%	2.0 $W·m^{-3}$	/	Optimized cultivation conditions for *Chlorella vulgar* enhance bioenergy recovery in MMFCs, where DO directly increases the output voltage and NH_4^+-N concentration indirectly affects it via DO.	[138]

Table 2. *Cont*.

Reactor Construction	Electrodes	Microalgal Species	Tape of Wastewater	Removal Rate (%)	Power Output	Biomass	Mechanisms	Refs.
Dual-chambered MMFC with AEM and PEM as separators	Anode: carbon brush; Cathode: Pt coated carbon cloth	*Chlorella vulgaris*	Simulated eutrophic water	15 h; COD: 94.5%; NH_4^+-N: 91.8%; NO_3^-: 90.6%; TP: 94.4%	8.27 kWh·m^{-3}	108.86 kJ·m^{-3}	Employing the self-generated electric field to drive and concentrate nutrient ions NO_3^--N and PO_4^{3-}-P in the anode and NH_4^+-N in the cathode, facilitating recovery as microalgal biomass.	[124]
Single chamber MMFC with an OCU	Anode: carbon felt; Air cathode electrode: AC/CB/PVDF/stainless steel mesh	*C. vulgaris*	Landfill leachate	COD: 86%; NH_4^+-N: 89.4%; NO_3^-: 90.6%; TN: 76.7%	/	89.3 mg; 1.23 g·L^{-1}·d^{-1}	The OCU's constraint of cathodic oxygen diffusion increases COD (16.72%) and NH_4^+-N (59.1%) removal, boosting algal biomass.	[123]
Algae-assisted triple-chamber MFC (one anodic chamber + two cathodic chambers)	Anode: carbon cloths; Cathode: carbon cloths	*Chlorella ap.* (FACHB-8)	Synthetic wastewater	8 days of total HRT; Cu^{2+}: 99.9%; TN: 79%	420 mW·m^{-2} (Cu^{2+} as electron acceptors) 315 mW·m^{-2} (O_2 as electron acceptors)	/	• Continuous flow operation mode realizes simultaneous removal of heavy metals, nutrients and organic matter; • Cu^{2+} and O_2 respectively act as electron acceptors for the reactions at the two cathodes.	[133]
Dual-chambered MMFC	Anode: carbon felt; Cathode: carbon felt	*Chlorella* (FACHB-8)	Simulated domestic wastewater	48 h of total HRT; COD: 84.62%; NH_4^+-N: 76.94%; TP: 76.94%; Chlortetracycline (240–260 μg·L^{-1}): 89.07%	13.39 W·m^{-3} (2-fold higher than the non-Fe^0)	/	• The continuous flow operation prevents anode acidification. • Fe^0 addition inhibits algal growth in the anode. • A synergistic anammox/Feammox mechanism enhances denitrification.	[120]
Single-chamber MMFC	Anode: graphite rod; Cathode: carbon mesh	Microalgae (*Scenedesmus almeriensis*)-bacteria (MB) consortia	Pig slurry	12 days; COD: 40–50%; NH_4^+-N: 100 %; TP: > 60%	153 mW·m^{-2}	0.069 g·L^{-1}·day^{-1}	• A cost-effective and durable ionic liquid-based membrane replaces conventional Nafion. • Microalgae-bacteria interactions enhance nutrient assimilation and recovery.	[128]
Polyethylene tubular-bag MMFC (10 L)	Anode: graphite felt; Cathode: graphite felt	*Chlorella vulgaris*	Synthetic wastewater	/	890 mW·m^{-3}	4.6 g·L^{-1}; 0.63 day^{-1}; • 0.307 kg·m^{-3}·d^{-1} algal productivity	• Algal lipids serve as the anode electron donor. A 10 L MFC employs rock phosphate-blended clayware (P source) and polyethylene bags as low-cost materials.	[25]

Note: OCU, bioactive oxygen consuming unit; AC/CB/PVDF, activated carbon/carbon black/polyvinylidene fluoride.

4. Synergistic Integration of Microalgae with Photocatalysis

Photocatalysis technology is an attractive alternative to other advanced oxidation technologies, due to its green energy characteristics, mild reaction conditions and the ability to produce rich free radical species. The artificial metal-based photocatalysts (such as TiO_2, WO_3, $BiVO_4$, BiOCl and ZnO) have been widely applied toward the removal of aqueous organic pollutants with high efficiency [139–141]. According to energy band theory, semiconductor photocatalysts possess discontinuous electronic structures, characterized by a valence band (VB) and a conduction band (CB) separated by a bandgap typically ranging from 1 to 4 eV [40] (Figure 5). Upon photon absorption, electrons are excited from the VB to the CB, creating electron-hole pairs. Photocatalytic degradation involves redox reactions occurring on the surface of semiconductors: (i) oxidative degradation via photoexcited

holes (h^+), and (ii) reduction reactions driven by photoexcited electrons, such as hydrogen evolution or oxygen reduction [142]. Upon light irradiation, photocatalysts generate abundant reactive species, including electrons, h^+, •OH, $•O_2^-$, and H_2O_2 [40]. Under the attack of these strong oxidants, organic compounds undergo ring opening and bond cleavage, ultimately transforming into biodegradable intermediates, CO_2 and H_2O [143]. However, the practical application of photocatalysis in pollutant removal is constrained by several challenges. Photocatalysts suffer from high recombination rates of photogenerated electron-hole pairs, often requiring the use of sacrificial agents [144]. Additionally, due to low mineralization efficiency or the need for extended irradiation to achieve high mineralization rates of organic pollutants, the reaction systems typically accumulate numerous intermediates, some of which may even exhibit greater toxicity than the original pollutants [39].

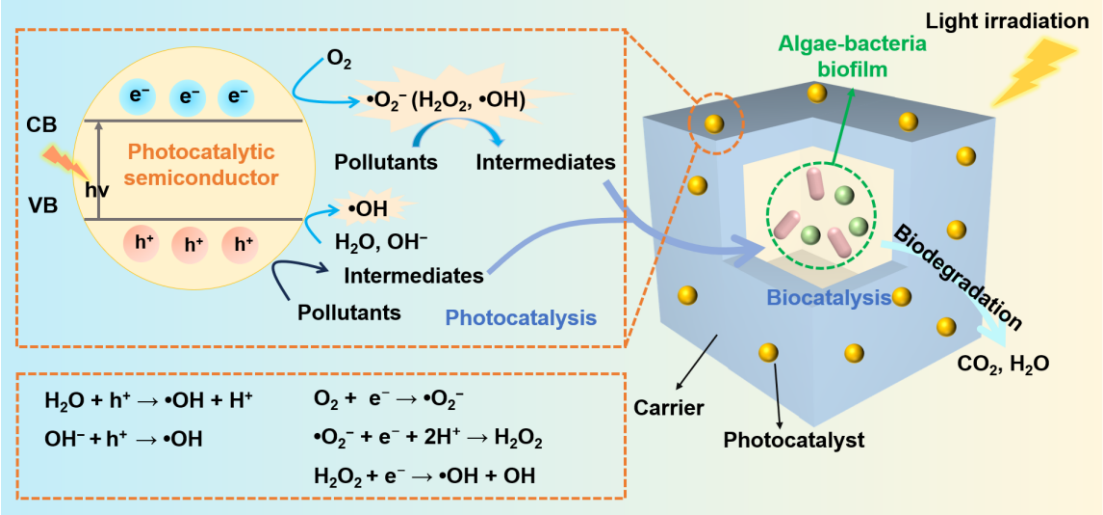

Figure 5. Schematic diagram of photocatalytic reaction mechanism and the synergistic effect between photocatalysts and microorganisms in the ICPB system.

Existing literature demonstrates that the combination of photocatalysis and microalgae technologies can enhance the removal rate of typical antibiotics and their photocatalytic degradation products, reducing their environmental risks. Photocatalytic nanoparticles such as $BiVO_4$ [44], g-C_3N_4 [39,42,145,146], TiO_2 [147,148], and the composites of metallic oxide [149,150] have been integrated with microalgae for pollutant remediation. Table 3 summarizes the removal efficiency of different wastewater by microalgae-photocatalysis coupling techniques. The coupling strategies generally fall into four categories: (i) sequential cascade degradation, with photocatalysis serving as a pretreatment step [151]; (ii) mixed system, where microalgae and photocatalytic nanoparticles are co-cultured in the same reactor [44]; (iii) nano-biohybrid system, where photocatalytic nanoparticles are coated on the microalgal biofilm by in situ synthesis or electrostatic adsorption [149,150]; (iv) intimately coupled photocatalysis and biodegradation (ICPB) system, where photocatalysts and microalgae are coated onto porous carriers or encapsulated in a hydrogel [152]. Chen et al. [44] integrated a monoclinic $BiVO_4$ with microalgae (*Dictyosphaerium* sp.) for visible-light-driven degradation of sulfamethazine. The $BiVO_4$–algae system demonstrated over 80% degradation within 4 days, primarily mediated by triplet-state dissolved organic matter (^{3}DOM*), followed by •OH. The $BiVO_4$ increased carbohydrate metabolites and activated the tricarboxylic acid cycle (TCA) of microalgae, significantly promoting the removal of sulfamethazine. However, the degradation mechanism was largely attributed to microalgal oxidative stress, resulting in relatively low degradation efficiency for antibiotics. The integration of microalgae with photocatalytic materials offers a promising approach for degrading and detoxifying organic pollutants, effectively reducing the environmental risks associated with typical antibiotics. Li et al. [151] found that the acute toxicity of norfloxacin (NOR) photocatalytic degradation by g-C_3N_4 increased because of the formation of many unmineralized products of NOR. The introduction of microalgae (*C. pyrenoidosa*) treatment promoted the degradation of some photocatalytic degradation products of NOR, and significantly reduced the overall toxicity of the treated solution.

However, there is a physical separation between the photocatalysts and microalgae, due to the harsh photocatalytic reaction conditions of g-C_3N_4 (UV light range, acidic pH). Shi et al. [145] combined the protonated graphitized carbon nitride (P-g-C_3N_4) with *Chlorella pyrenoidosa* through electrostatic adsorption to form a new photocatalytic-microalgae composite system. *Chlorella pyrenoidosa* enhanced the photocatalytic activity of P-g-C_3N_4 through extracellular organic matters (EOMs) photosensitization and electron transfer, and there was a synergistic effect between P-g-C_3N_4 and microalgae, which realized the efficient degradation and mineralization

of tetracycline hydrochloride (TCH). $\bullet O_2^-$ plays the crucial function in the degradation of TCH in this system. Besides, Mao et al. [42] found that P-g-C_3N_4 induced moderate oxidative stress in algae. The metabolic adaptation facilitated the formation of extracellular polymeric substances (EPS) for resisting the physiological damage caused by toxic substances in water. The generation of oxidative $\bullet O_2^-$ by acclimated algae contributed to over five-fold enhancement in the degradation of harmful aniline. Besides, many studies reported that the intimate interaction between microalgae and photocatalysts could facilitate the degradation efficiency [149]. Zhang et al. [150] developed a visible-light-driven nano-biohybrid system (*C. ellipsoidea*@TiO_2-Ag-AgCl) via biomimetic synthesis for efficient o-cresol biodegradation. This system achieved a biodegradation rate of 5.56 mg L^{-1} h^{-1}, representing a 6.49- and 3.66-fold enhancement over native microalgae and catalysts alone, and surpassing TiO_2-modified systems (3.57 mg L^{-1} h^{-1}). Such a hybrid system could improve electron transfer within microalgae, promoting the TCA cycle-driven mineralization of intermediates and accelerating the overall biodegradation process [150]. Moreover, photocatalyst nanoparticles provided protective effects against pollutant toxicity by increasing chlorophyll a content, stimulating EPS secretion, and improving membrane permeability. All these processes enabled microalgae to adapt more quickly to the toxic environment.

Due to the difficulty in matching the cultivation conditions of microalgal cells with photocatalytic systems, or cells' susceptibility to inactivation by the high ROS around photocatalysts, the ICPB system has been proposed [153]. In this system, both photocatalysts and microalgae are immobilized together onto porous carriers. An ICPB system typically comprises four essential components: porous carriers, photocatalysts, biofilms, and an illuminated reactor, as shown in Figure 5 [154]. In ICPB, AOPs and biodegradation occur simultaneously in the same reactor: photocatalysts on the carrier surface convert refractory pollutants into biodegradable intermediates, which are then completely degraded by the nearby algae-bacterial biofilm communities cultivated in the carriers. Additionally, the biofilms are protected by the carriers from the harmful light and free radicals generated by photocatalysts [155]. ICPB has demonstrated promising applicability for the degradation of various bio-recalcitrant pollutants, such as phenolics, pharmaceuticals, and endocrine disrupters [34,156–159].

In ICPB systems, two primary methods are employed to integrate photocatalysts, carriers, and biofilms. The first involves coating photocatalysts onto porous carriers (e.g., ceramic particles, biochar hydrogel, polyurethane sponge, photocatalytic optical hollow fibers) [154,157,160,161]. Sometimes, polydopamine was applied as an adhesive layer to strengthen the attachment of photocatalysts to the carriers [162]. These coated carriers are then incubated with microbial media to promote biofilm growth within the pores. The second method entails dispersing both photocatalysts and microorganisms in sodium alginate, which is then added dropwise into a $CaCl_2$ solution to form calcium alginate beads [163]. Both approaches protect microorganisms from UV light and free radicals, while ensuring close contact between photocatalysts and biofilms. This construction facilitates efficient transfer of photodegradation products to microbes, improving secondary mineralization.

Table 3. Applications of microalgae-photocatalysis hybrid systems for the degradation of pollutants.

System	Material Composition	Microorganism	Light Source	Target Pollutants or Wastewater	Degradation Performance	Refs.
ICPB	Photocatalyst: TiO_2@FeS_2; Carrier: Polyether-type polyurethane-graphene oxide (GO-PP) sponges in a 1 cm^3 scale	Algae-bacteria consortia system	A 7 W LED strip (1 m long with 50 light beads) in batch mode	Coking wastewater	· Composites: COD (55.6%), TOC (58.2%), and TN (30.4%) over 2 h; · Biodegradation: COD (24.8%), TOC (28.8%), and TN (5.3%) over 2 h	[160]
ICPB	GeO_2/Zn-HPW/TiO_2-loaded (HPW = phosphotungstic acid hydrate) photocatalytic optical hollow fibers (POHFs)	Algal-bacterial biofilm (*Scenedesmus obliquus*, *Salinarimonas*, *Coelastrella* sp., and *Rhizobium*)	A deuterium halide light source in 190–2000 nm range	Tetracycline	98.1% in 5 h; 95.0% of COD in 10 h (8.82 μmol·h^{-1})	[151]
ICPB	N-doped TiO_2 (NT)-coated POHFs	*Scenedesmus obliquus*	A UV−vis LED light source (300–850 nm)	2.12 mM phenol	· Composites: 100% in 14 h; ~99% of TOC in 24 h; · Photocatalysts: 100% in 34 h; 70% of TOC in 34 h · Biodegradation: 100% in 28 h; 96% of TOC in 28 h	[37]

Table 3. *Cont.*

System	Material Composition	Microorganism	Light Source	Target Pollutants or Wastewater	Degradation Performance	Refs.
Mixed system	0.5 g·L^{-1} $BiVO_4$–algae system	100 mg L^{-1} *Dictyosphaerium* sp.	4000 lux illumination with a light-dark period of 12:12 h.	5 mg·L^{-1} sulfamethazine	· 83% for composites in 4 days; · 34% for $BiVO_4$ in 4 days; · 41% for algae in 4 days	[44]
Mixed system	0.1 g·L^{-1} protonated g-C_3N_4 (P-C_3N_4)	*Microcystis aeruginosa*	A 4000 lux cool white fluorescent, with a light-dark period of 14:10 h.	1 g·L^{-1} aniline	· 96% in 48 h for composites · 0.14 h^{-1} for composites; · 0.005 h^{-1} for P-C_3N_4; · 0.024 h^{-1} for biodegradation	[42]
Mixed system	0.2 g·L^{-1} P-g-C_3N_4	5.0 × 10^8 cells mL^{-1} *Chlorella pyrenoidosa*	350 W xenon lamp (400 nm–780 nm) to simulate visible light	10 mg·L^{-1} tetracycline hydrochloride	· 53% in 2 h. · The k_{obs} of algae, P-g-C_3N_4, and P-g-C_3N_4/algae increased to 0.012 min^{-1}, 0.0029 min^{-1}, and 0.0061 min^{-1}, respectively.	[145]
			350 W xenon lamp (290 nm–780 nm) to simulate sunlight		· 100% in 2 h. · The k_{obs} of algae, P-g-C_3N_4, and P-g-C_3N_4/algae increased to 0.003 min^{-1}, 0.027 min^{-1}, and 0.038 min^{-1}, respectively.	
Mixed system	TiO_2/graphene oxide/polypropylene fiber	*Chlorella pyrenoidosa*	A light incubator (2000 lux) with a light/dark period of 12/12 h.	5 mg·L^{-1} roxithromycin (ROX)	· Composites: 91.73% in 14 days. · Biodegradation: 14.45% in 14 days. · Photocatalysts: 70.95% in 14 days.	[149]
Nano-biohybrid system	*C. ellipsoidea*@TiO_2-Ag-AgCl system	*C. ellipsoidea*	A light incubator (4500 lux) in a light-dark period of 16/8 h.	100 mg·L^{-1} o-cresol	· Composites: 100% in 18 h (3.57 mg L^{-1}·h^{-1}) · Biodegradation: 20 % in 28 h (0.857 mg L^{-1}·h^{-1}) · Photocatalysts: 42.7 % in 28 h (1.52 mg L^{-1}·h^{-1}).	[150]
Nano-biohybrid system	Biosynthetic TiO_2 (bio-TiO_2 NPs)—microalgae synergetic system (Bio-TiO_2/Algae complex)	*Tetradesmus obliquus*	A light incubator (4500 lux) with a light/dark period of 16/8 h.	100 mg·L^{-1} phenol	· Composites: 98.95% in 19 h. · Biodegradation: 40.88% in 19 h. · Dead Algae + bio-TiO_2: 74.89% in 19 h.	[164]

To enhance photocatalytic degradation, ICPB systems require high light transmittance, broad light absorption, and low charge carrier recombination. Yuan et al. [37] demonstrate a novel ICPB system using N-doped TiO_2-coated photocatalytic optical hollow fibers (POHFs) in cooperation with *Scenedesmus obliquus* biofilm for phenol removal. The N-TiO_2-POHFs exhibited high UV−visible photocatalytic activity, enabling rapid phenol removal while emitting visible light to sustain biofilm growth and O_2 production. O_2 generated by algae as an electron acceptor was transferred to the surface of POHFs, suppressing electron-hole recombination and promoting ROS generation (•OH and $•O_2^-$). To further improve the optical characteristics of the carriers, Xiao et al. [151] fabricated GeO_2/Zn-HPW/TiO_2-loaded (POHFs) (HPW = phosphotungstic acid hydrate) with a broad absorption edge extending to 1000 nm, which provided high light intensity to support biofilm growth. The algal-bacterial biofilm supplied O_2 required for photocatalysis, while biodegradation reduced ROS consumption by organics, synergistically enhancing photocatalytic efficiency. Consequently, this ICPB system achieved 98.1% tetracycline removal within 5 h and 95.0% mineralization in 10 h, along with an 11-fold increase in biofilm biomass.

The microalgae-based ICPB system has been effectively applied to real refractory industrial wastewater. Zhu et al. [160] developed an *in situ* immobilized photocatalytic-algae-bacteria consortia (P-ABC) system using a polyether polyurethane sponge carrier for actual coking wastewater treatment. Partially embedded photocatalysts formed isolated “photocatalytic islands” alongside “biological islands”, which minimized direct contact and oxidative damage to microbes while promoting biofilm growth and system stability. The P-ABC system increased algal density by 16.8% and significantly improved the removal efficiencies of COD (19.8%), TOC (21.2%), and TN (30.4%) compared to conventional bio-systems.

5. Synergistic Integration of Microalgae with Electrochemical Advanced Oxidation Processes (EAOPs)

To enhance the removal efficiency of refractory organic contaminants, the integration of microalgae-based systems with EAOPs has been proposed [165]. EAOPs have been widely employed for treating refractory pollutants because they rely on electricity to produce the strong oxidants, mainly •OH radicals (E = 2.8 V vs. SHE), which can non-selectively degrade/mineralize organic matters [166]. Moreover, EAOPs offer the advantage of producing minimal secondary sludge or waste, thereby reducing post-treatment demands, and electrochemical reactors are readily automated. •OH can be produced directly via anodic oxidation of water (electrochemical oxidation, EO), and can also be generated indirectly through Fenton's reagent (electro-Fenton) reactions at the cathode [20]. Among various EAOPs, the electro-Fenton process has attracted considerable attention due to its ability to continuously generate H_2O_2 through the two-electron ORR using cost-effective carbon-based materials [167,168]. In the presence of Fe^{2+} ions, H_2O_2 undergoes the Fenton reaction to form •OH, which is maintained through the continuous regeneration of Fe^{2+} at the cathode via the reduction of Fe^{3+} [169]. However, the practical application of EAOPs may be expensive due to the extended electrolysis time required for complete contaminant mineralization, leading to high energy consumption [170]. Consequently, hybrid treatments integrating biological processes with EAOPs have emerged as promising alternatives to enhance pollutant removal while lowering the operational costs associated with EAOPs [171,172]. In particular, EAOPs have been proposed as a pretreatment step prior to conventional biological treatment [173]. By partially oxidizing refractory or toxic organic compounds, EAOPs can significantly improve the biodegradability of wastewater. This integrated approach not only shortens the treatment time required by EAOPs but also lowers the overall energy consumption. Table 4 presents the recent studies of microalgae-EAOPs hybrid systems for the degradation of pollutants.

The presence of insoluble particles and dark-colored substances in anaerobic effluent often limits light penetration, thereby inhibiting microalgal growth. The Electro-Fenton process offers a promising pretreatment method to condition such wastewater for subsequent microalgal cultivation. Huo et al. [38] combined H_2O_2-enhanced electro-Fenton coagulation (EFC) with microalgae for the treatment of anaerobic digestion sludge. The EFC pretreatment significantly improved light availability and enhanced photosynthesis in *Chlorella* sp. However, it also resulted in considerably reduced pH, requiring neutralization prior to algal cultivation. Furthermore, while electro-Fenton effectively oxidizes organic pollutants, inorganic species are often transformed rather than completely removed, and thus remain in the treated effluent. Microalgae can assimilate these residual inorganics as well as biodegradable organics, offering a complementary treatment step. Dulce María Arias [36] combined EF and microalgae in a two-step integrated process to treat high-load industrial wastewater. EF pretreatment reduced COD by 77.5%, total suspended solids (TSS) by > 95%, and PO_4^{3-} by 74.3% at 6.32 mA cm^{-2}, decreasing the turbidity and enhancing biodegradability. Subsequent microalgal cultivation removed 85% of residual organics, all inorganic N and P, and 65% of residual Fe within 15 days. However, the effectiveness of EO processes as a pretreatment depends heavily on wastewater composition [112]. Eliana M. Jiménez-Bambague et al. [172] demonstrated that using EO as a post-treatment after microalgae in bench-scale tests resulted in superior removal of pharmaceuticals (58.8% vs. 47.7%) and COD (63% vs. 24.3%) compared to EO as pretreatment during pharmaceuticals wastewater treatment. This improvement was attributed to the prior consumption of biodegradable substances by microalgae, which would otherwise scavenge •OH during EO. Based on these results, a pilot-scale high-rate algal pond (HRAP)-EO system was then implemented, removing over 80% of key pharmaceuticals.

The approach described above employs a sequential microalgae-EAOP treatment cascade, as the harsh operating conditions required by EAOPs prevent microalgae from surviving in a shared system. As a result, this configuration fails to leverage the synergistic effects of simultaneous microalgae and EAOP treatment. Microalgal bioelectrochemical oxidation offers a promising self-powered approach for the *in situ* activation of peroxymonosulfate (PMS), enabling simultaneous activation and contaminant removal [174]. For example, microalgae can act as an electron donor in the anode of MMFCs to generate electricity through the photosynthetic electron-transfer chain [175], which can activate PMS and achieve the combination of green bioelectricity and PMS-based AOPs for sustainable pollutants degradation. Deng et al. [176] constructed a dual-chamber microalgae fuel cell using microalgae as the anode electron donor and PMS as the cathode electron acceptor. Under closed-circuit conditions, 1–12 mM PMS was activated, achieving 32.00–99.83% sulfamethoxazole (SMX) degradation within 24 h, 1.21–1.78 times higher than in open-circuit mode. The process involved key reactive species such as $•SO_4^-$, •OH, and $^1O_2$.

The integration of microalgae and EAOPs presents a promising, hybrid approach for removing both heavy metals and persistent organic pollutants from highly contaminated effluents, as evidenced by its successful progression to pilot-scale studies. Strategically sequencing the treatment steps (EAOPs serve as either pre-

treatment or post-treatment) should be based on wastewater composition. Future efforts should focus on intensifying EAOPs' efficiency and cost-effectiveness. More active oxidants (e.g., peroxymonocarbonate and peracetic acid) could be employed as the cathode electron acceptors in advanced microalgae-based self-powered systems to enhance the removal efficiency.

Table 4. Applications of microalgae-EAOPs hybrid systems for the degradation of pollutants.

Material Composition	Microorganism	Target Pollutants/Wastewater	Treatment Process	Time	Removal Rate	Energy Consumption	Refs.
A pair of BDD/BDD electrodes	*Scenedesmus* sp.	Pharmaceutical compounds (at bench scale)	Electrooxidation as a post-treatment, microalgae as a pre-treatment (MA/EO process)	1 h of EO + 7 days of microalgae treatment	COD: 63%; Pharmaceutical compounds removal: 58.8%	0–30 V, 10 $mA \cdot cm^{-2}$	[172]
		Pharmaceutical compounds (at pilot scale, 50 L)	MA/EO process	3 days of microalgae treatment + 1 h of EO	COD: 57.4%; Pharmaceutical compounds removal: 36.8–94.3%	0.28–1.02 $kWh \cdot m^{-3}$	[172]
A pair of iron–iron plate electrodes	*Chlorella*	Anaerobic digestion wastewater	Fe-H_2O_2-EFC as a pre-treatment, microalgae as a post-treatment	2.5 min of EFC + 20 days of microalgae treatment	COD: 87.3%; Color: 80.8%; TSS: 79.5%	0.26~0.69 $kWh \cdot m^{-3}$	[38]
Ti/RuO_2–IrO_2 anode; Carbon felt cathode	*Scenedesmus* sp., *Chlorosarcinopsis* sp., and *Coelastrum* sp.	Food processing wastewater	EF process as a pre-treatment, microalgae as a post-treatment	6 h of EF + 15 days of microalgae treatment	EF: COD: 77.5%; TSS: >95%; TP: 74.3%; TN: 76.9%; EF-Microalgae: COD: 91.0%; TN: 100%; TP: 100%	0.04 $kWh \cdot g^{-1} \cdot COD^{-1}$	[36]
Ti/$(RuO_2)_{0.9}(TiO_2)_{0.1}$ anode; Stainless steel 316 cathode	*Chlorella sorokiniana* UNSA-2	Tannery wastewater	MA/EO process	18 days of microalgae treatment + 1 h of EO	COD: 94.25% Cr: 78.43%; As: 99.3 %; V: 98.9 %	21.4 $kWh \cdot m^{-3}$	[177]
A pair of carbon papers electrodes	*Scenedesmus* sp. TXH	20 μM SMX	Microalgae in anode for bio-electricity generation: PMS as the electron acceptor in cathode and microalgae as biocatalysts in anode	24 h	Close–circuit: 99.83% COD; Open–circuit: 65% COD	Power output: 700 $mW \cdot m^{-3}$	[176]

Note: Fe-H_2O_2-EFC, Fe electrode with H_2O_2-enhanced electro-Fenton coagulation; EF, electron-Fenton. MA, microalgae; EO, electrooxidation; SMX, sulfamethoxazole.

6. Summary, Challenges, and Research Outlook

Microalgae have emerged as promising agents for bioremediation, particularly in wastewater treatment, owing to their capacity for nutrient removal and biomass valorization. Nevertheless, their ability to degrade certain recalcitrant pollutants and treat complex wastewater compositions remains limited. In recent years, several hybrid technologies integrating microalgal systems have been explored to overcome these constraints, including microalgal microbial fuel cells (MMFCs), microalgae coupled with electrochemical advanced oxidation processes (EAOPs), and microalgae integrated with photocatalysis. Compared to standalone bioremediation, bioelectrochemical systems, or electrochemical/photocatalytic-based AOPs, these combined approaches have achieved synergistic enhancement in pollutant removal performance. However, most remain at an early developmental stage, with limited mechanistic understanding of the operational processes. AOPs based on free radicals, such as electro-Fenton (EF) reactions and photocatalysis, are particularly effective for refractory pollutants, but they face challenges including the formation of toxic intermediates, strong dependence on controlled pH conditions, and interference from coexisting substances.

6.1. Microalgal Microbial Fuel Cells

Although numerous studies have reported the use of MMFCs for treating real wastewater, large-scale MMFC research remains limited [25]. The pilot-scale scaling of MMFCs faces a major cost challenge, as membranes and electrodes can comprise over 80% of the total cost [21,178]. Additionally, prolonged operation time, coupled with a lack of suitable monitoring equipment, leads to high maintenance costs. Scaling up the system also results in increased internal resistance, reduced mass transfer efficiency, and lower power generation efficiency.

To enhance feasibility, techno-economic assessments (TEA) and energy flow analyses are crucial. A comprehensive evaluation should incorporate costs related to electrodes, reactor construction, energy input, and biomass extraction, alongside revenues from electricity, biomass, and wastewater treatment services [138]. A comprehensive energy flow analysis that considers energy inputs (such as pumping, illumination, and biodiesel processing) and outputs (including electricity and biodiesel) is essential for evaluating feasibility. Reports indicate that electricity generation contributes only 12.7–42.3% of total energy consumption (excluding biodiesel processing), while biodiesel-derived energy represents 27.3–32.9%, which is required to achieve energy neutrality and offset economic costs [122]. Moreover, to reduce the capital cost of MMFCs, it is crucial to adopt low-cost electrodes and membranes. Promising alternatives include earthen ceramic membranes [179] and polymer inclusion membranes (PIMs) [128], which can replace expensive materials like methyltrioctylammonium chloride and minimize the cost of periodic replacement [24]. Furthermore, the development of high-performance, biomass-derived ORR catalysts offers a pathway to cost-effective cathodes.

In terms of pollutant removal, the slow biodegradation rate of MMFCs necessitates optimization of operational parameters such as strain selection, light intensity, temperature, nutrient supply, and cultivation systems, with artificial neural network (ANN) modelling and forensic-based investigation algorithm (FBI) offering possible solutions [180]. Integration with complementary methods, including algal–bacterial symbiosis [181,182], membrane filtration [183], and photocatalysis [184], has demonstrated improved overall efficiency. Notably, hybrid photocatalytic–electrogenic anodes have shown enhanced extracellular electron transfer and higher pollutant removal [185,186], suggesting photocatalysis-assisted MMFC as a cost-effective and efficient strategy.

6.2. Microalgae Integrated with Photocatalysis System

Microalgae integrated with photocatalysis also face key challenges: notably, rapid photogenerated charge recombination, narrow visible-light absorption, and insufficient integration with biofilms. Addressing these issues requires the design of heterojunction photocatalysts with broad spectral response [187], high interfacial conductivity [188], and high charge separation efficiency to facilitate direct electron transfer between catalysts and biofilms. Tightly coupled hybrid systems, such as in situ mineralization of photocatalytic nanomaterials on microalgal biofilms, may further strengthen material–biological synergy. However, detailed mechanistic understanding of photocatalyst–biofilm interactions, especially photoelectron transfer processes and their impact on ICPB systems, remains lacking [188]. Omics technologies, including transcriptomics, proteomics, and metabolomics, can elucidate functional genes, proteins, and enzymes involved in pollutant degradation pathways within dynamic microbial communities [189]. Moreover, poor adhesion between photocatalysts and substrates compromises recyclability, highlighting the need for low-cost carrier materials with high stability, strong light transmittance, and large specific surface area, alongside optimized immobilization methods to secure durable loading of both photocatalysts and biofilms.

Microalgae-coupled photocatalysis has gained notable development in recent years, owing to its simple configuration, low energy input, cost-effectiveness, and efficient degradation capability. However, most current research remains confined to laboratory-scale studies, primarily utilizing low-concentration antibiotics and a specific pollutant as model pollutants. This limitation has prevented adequate pilot-scale validation of the technology's long-term performance under realistic conditions. Scaling up the system necessitates the design of larger reactors that achieve efficient mass transfer while maintaining uniform light distribution, which demands complex geometries and substantial energy input for effective mixing.

6.3. Microalgae Integrated with EAOPs Systems

For microalgae–EAOP systems, particularly the EF process, operational limitations include the requirement for external H_2O_2 and Fe^{2+} additions, acidic conditions leading to effluent acidification and necessitating neutralization, interference from complex water matrices, and physical separation between EAOPs and microalgal components that diminishes synergy. Development of heterogeneous electro-Fenton (HEF) catalysts is a promising approach [190], enabling in situ H_2O_2 generation through the two-electron ORR at carbon-based cathodes, followed by activation into •OH via solid-Fenton catalysts [191]. HEF systems avoid external H_2O_2 addition,

reduce iron sludge formation, attenuate pH sensitivity, and allow catalyst recovery. In addition, their long-term stability can be achieved by structural designs that confine catalytic sites, enhance Fe^{2+}/Fe^{3+} cycling, and limit metal leaching [192]. Additionally, coupling hydrogel-immobilized microalgae with O_2-dependent AOPs in a single reactor can protect cells from ROS damage, permit nutrient/gas exchange, and facilitate cell cultivation and harvesting [193]. Moreover, the enhanced mechanical strength and biocompatibility of encapsulation materials (e.g., modified alginate) are essential to prevent cell leakage and sustain long-term cell viability [194]. Furthermore, microalgal bioelectricity offers opportunities for in situ activation of PMS, where improved electron transfer efficiency via porous conductive polymers or redox mediators could significantly boost current density and voltage output [195].

The microalgae-coupled EAOPs system has been extensively reported for its effective treatment of complex, real wastewater in large-scale configurations, demonstrating the most outstanding remediation capability among the three technologies in practical applications. Nevertheless, it remains the most expensive option, with costs encompassing not only the electrochemical oxidation unit but also energy consumption, post-treatment processes, and the extended cultivation of microalgae. These high costs currently hinder its widespread large-scale adoption. Additionally, few studies have provided a comprehensive techno-economic evaluation of this system, underscoring the need for greater focus on its economic viability in future research.

In summary, forthcoming studies should move beyond seeking incremental gains in operational efficiency and instead pursue the development of microalgae–hybrid systems that maintain stable performance under variable wastewater compositions and environmental conditions. This will require not only advances in reactor configurations and process integration, but also the incorporation of responsive monitoring and control strategies capable of adjusting operational parameters in real time. Addressing the treatment of complex wastewater is particularly critical, as large fluctuations in pollutant load, coexisting ions, and pH can destabilize system performance. To underpin these advances, detailed investigations of the interplay between microalgae and engineered processes are needed, covering both molecular-level phenomena—such as electron transfer pathways, radical generation dynamics, and metabolite transformations—and system-level behaviour under realistic operating conditions. Coupling multi-omics analyses with electrochemical measurements and high-resolution imaging can provide key mechanistic insights. Parallel to technical development, a comprehensive evaluation framework should be applied to assess effluent toxicity, potential secondary pollution, and broader environmental trade-offs, drawing on energy flow analysis, TEA, and carbon footprint evaluation. Quantifying the benefits of resource recovery, particularly from algal biomass used in biofuels or high-value products, is essential for achieving significant cost recovery in scaled-up systems. By integrating a mechanistic understanding with adaptive operation and robust sustainability assessment, microalgae–hybrid systems can be advanced towards practical, scalable, and economically sustainable deployment for real-world wastewater treatment.

Funding

This research received no external funding.

Conflicts of Interest

The authors declare no conflict of interest.

Use of AI and AI-assisted Technologies

No AI tools were utilized for this paper.

References

1. Deshmukh, M.K.G.; Sameeroddin, M.; Abdul, D.; et al. Renewable energy in the 21st century: A review. *Mater. Today Proc.* **2023**, *80*, 1756–1759.
2. Shahid, M.K.; Kashif, A.; Fuwad, A.; et al. Current advances in treatment technologies for removal of emerging contaminants from water—A critical review. *Coord. Chem. Rev.* **2021**, *442*, 213993.
3. Jones, E.R.; van Vliet, M.T.H.; Qadir, M.; et al. Country-level and gridded estimates of wastewater production, collection, treatment and reuse. *Earth Syst. Sci. Data* **2021**, *13*, 237–254.
4. Zhao, C.; Chen, H.; Song, Y.; et al. Electricity production performance enhancement of microbial fuel cells with double-layer sodium alginate hydrogel bioanodes driven by high-salinity waste leachate. *Water Res.* **2023**, *242*, 120281.
5. Goliopoulos, N.; Mamais, D.; Noutsopoulos, C.; et al. Energy consumption and carbon footprint of Greek wastewater treatment plants. *Water* **2022**, *14*, 320.

6. Liu, R.; Ma, Y.; Zhang, H.; et al. A review-based estimation of GHG emissions of China's wastewater management system. *J. Environ. Manag.* **2025**, *380*, 124869.
7. Guo, Y.; Askari, N.; Smets, I.; et al. A review on co-metabolic degradation of organic micropollutants during anaerobic digestion: Linkages between functional groups and digestion stages. *Water Res.* **2024**, *256*, 121598.
8. Krzeminski, P.; Tomei, M.C.; Karaolia, P.; et al. Performance of secondary wastewater treatment methods for the removal of contaminants of emerging concern implicated in crop uptake and antibiotic resistance spread: A review. *Sci. Total Environ.* **2019**, *648*, 1052–1081.
9. Gasana, Z.; Kayiranga, A.; Nizeyimana, J.C.; et al. Removal of antibiotics and antibiotic resistance genes using microalgae-based wastewater treatment system: A bibliometric review and mechanism analysis. *J. Water Process Eng.* **2025**, *72*, 107496.
10. Mehariya, S.; Das, P.; Thaher, M.I.; et al. Microalgae: A potential bioagent for treatment of emerging contaminants from domestic wastewater. *Chemosphere* **2024**, *351*, 141245.
11. Xiong, Q.; Hu, L.-X.; Liu, Y.-S.; et al. Microalgae-based technology for antibiotics removal: From mechanisms to application of innovational hybrid systems. *Environ. Int.* **2021**, *155*, 106594.
12. Sutherland, D.L.; Ralph, P.J. Microalgal bioremediation of emerging contaminants—Opportunities and challenges. *Water Res.* **2019**, *164*, 114921.
13. Pandey, S.; Narayanan, I.; Selvaraj, R.; et al. Biodiesel production from microalgae: A comprehensive review on influential factors, transesterification processes, and challenges. *Fuel* **2024**, *367*, 131547.
14. Kumar, D.; Singh, B.; Sharma, Y.C. Challenges and opportunities in commercialization of algal biofuels. In *Algal Biofuels*; Gupta, S., Malik, A., Bux, F., Eds.; Springer: Cham, Switzerland, 2017. https://doi.org/10.1007/978-3-319-51010-1_20.
15. Xiong, W.; Peng, Y.; Ma, W.; et al. Microalgae–material hybrid for enhanced photosynthetic energy conversion: A promising path towards carbon neutrality. *Natl. Sci. Rev.* **2023**, *10*, nwad200.
16. Khan, T.A.; Liaquat, R.; Zeshan; et al. Biological carbon capture, growth kinetics and biomass composition of novel microalgal species. *Bioresour. Technol. Rep.* **2022**, *17*, 100982.
17. Koyande, A.K.; Chew, K.W.; Rambabu, K.; et al. Microalgae: A potential alternative to health supplementation for humans. *Food Sci. Hum. Wellness* **2019**, *8*, 16–24.
18. You, X.; Yang, L.; Zhou, X.; et al. Sustainability and carbon neutrality trends for microalgae-based wastewater treatment: A review. *Environ. Res.* **2022**, *209*, 112860.
19. Leng, L.; Wei, L.; Xiong, Q.; et al. Use of microalgae based technology for the removal of antibiotics from wastewater: A review. *Chemosphere* **2020**, *238*, 124680.
20. Zheng, S.; Wang, Y.; Chen, C.; et al. Current progress in natural degradation and enhanced removal techniques of antibiotics in the environment: A review. *Int. J. Environ. Res. Public Health* **2022**, *19*, 10919.
21. Montoya-Vallejo, C.; Quintero Díaz, J.C.; Yepes, Y.A.; et al. Microalgal microbial fuel cells: A comprehensive review of mechanisms and electrochemical performance. *Appl. Sci.* **2025**, *15*, 3335.
22. Anandapadmanaban, B.H.; Liu, S.-H.; Lin, C.-W. Prospects of microalgae in the cathode chamber of microbial fuel cells: From sequestration to bioproduct production. *Biomass Bioenergy* **2025**, *194*, 107616.
23. Wang, X.; Hong, Y.; Zhang, Y. Photosynthetic algal microbial fuel cell (PAMFC) for wastewater removal and energy recovery: A review. *Curr. Pollution. Rep.* **2023**, *9*, 359–373.
24. Jaiswal, K.K.; Kumar, V.; Vlaskin, M.S.; et al. Microalgae fuel cell for wastewater treatment: Recent advances and challenges. *J. Water Process Eng.* **2020**, *38*, 101549.
25. Khandelwal, A.; Chhabra, M.; Yadav, P. Performance evaluation of algae assisted microbial fuel cell under outdoor conditions. *Bioresour. Technol.* **2020**, *310*, 123418.
26. Nagendranatha Reddy, C.; Nguyen, H.T.H.; Noori, M.T.; et al. Potential applications of algae in the cathode of microbial fuel cells for enhanced electricity generation with simultaneous nutrient removal and algae biorefinery: Current status and future perspectives. *Bioresour. Technol.* **2019**, *292*, 122010.
27. Wang, X.; Xie, J.-F.; Zhao, Q.-B.; et al. Self-supported antimony tin oxide anode with Sb segregation promoted atrazine removal. *J. Mater. Chem. A* **2024**, *12*, 27206–27211.
28. Isaev, A.B.; Shabanov, N.S.; Magomedova, A.G.; et al. Electrochemical oxidation of azo dyes in water: A review. *Environ. Chem. Lett.* **2023**, *21*, 2863–2911.
29. Heidari, Z.; Pelalak, R.; Zhou, M. A critical review on the recent progress in application of electro-Fenton process for decontamination of wastewater at near-neutral pH. *Chem. Eng. J.* **2023**, *474*, 145741.
30. Zhao, N.; Zhang, J.; Cao, F.; et al. Electro-Fenton purification of floodwater with a poly(vinyl alcohol)-treated $FeNi_3$@laser-induced 3D-graphene composite anode from Kraft paper. *Chem. Eng. J.* **2025**, *503*, 158206.
31. Khader, E.H.; Muslim, S.A.; Saady, N.M.C.; et al. Recent advances in photocatalytic advanced oxidation processes for organic compound degradation: A review. *Desalin. Water Treat.* **2024**, *318*, 100384.

32. Krishnan, A.; Swarnalal, A.; Das, D.; et al. A review on transition metal oxides based photocatalysts for degradation of synthetic organic pollutants. *J. Environ. Sci.* **2024**, *139*, 389–417.
33. Jain, B.; Singh, A.K.; Kim, H.; et al. Treatment of organic pollutants by homogeneous and heterogeneous Fenton reaction processes. *Environ. Chem. Lett.* **2018**, *16*, 947–967.
34. Xiangyu, B.; Chao, L.; Shilong, H.; et al. Combining advanced oxidation processes with biological processes in organic wastewater treatment: Recent developments, trends, and advances. *Desalin. Water Treat.* **2025**, *323*, 101263.
35. Almaguer, M.A.; Cruz, Y.R.; Da Fonseca, F.V. Combination of advanced oxidation processes and microalgae aiming at recalcitrant wastewater treatment and algal biomass production: A review. *Environ. Process.* **2021**, *8*, 483–509.
36. Arias, D.M.; Olvera Vargas, P.; Vidal Sánchez, A.N.; et al. Integrating electro-Fenton and microalgae for the sustainable management of real food processing wastewater. *Chemosphere* **2024**, *360*, 142372.
37. Yuan, J.; Chen, M.; Xiang, W.; et al. Rapid and sustainable conversion of phenol to microalgae biomass. *ACS Sustain. Chem. Eng.* **2021**, *9*, 16182–16191.
38. Huo, S.; Necas, D.; Zhu, F.; et al. Anaerobic digestion wastewater decolorization by H_2O_2-enhanced electro-Fenton coagulation following nutrients recovery via acid tolerant and protein-rich *Chlorella* production. *Chem. Eng. J.* **2021**, *406*, 127160.
39. Li, C.; Tian, Q.; Zhang, Y.; et al. Sequential combination of photocatalysis and microalgae technology for promoting the degradation and detoxification of typical antibiotics. *Water Res.* **2022**, *210*, 117985.
40. Zuo, W.; Zhang, L.; Zhang, Z.; et al. Degradation of organic pollutants by intimately coupling photocatalytic materials with microbes: A review. *Crit. Rev. Biotechnol.* **2021**, *41*, 273–299.
41. Costa, I.G.F.; Terra, N.M.; Cardoso, V.L.; et al. Photoreduction of chromium(VI) in microstructured ceramic hollow fibers impregnated with titanium dioxide and coated with green algae *Chlorella vulgaris*. *J. Hazard. Mater.* **2019**, *379*, 120837.
42. Mao, J.; Gu, Z.; Zhang, S.; et al. Protonated carbon nitride elicits microalgae for water decontamination. *Water Res.* **2022**, *222*, 118955.
43. Abdelfattah, A.; Ali, S.S.; Ramadan, H.; et al. Microalgae-based wastewater treatment: Mechanisms, challenges, recent advances, and future prospects. *Environ. Sci. Ecotechnol.* **2023**, *13*, 100205.
44. Chen, S.; Yuan, M.; Feng, W.; et al. Catalytic degradation mechanism of sulfamethazine via photosynergy of monoclinic $BiVO_4$ and microalgae under visible-light irradiation. *Water Res.* **2020**, *185*, 116220.
45. Ji, J.; Li, H.; Liu, S. Current natural degradation and artificial intervention removal techniques for antibiotics in the aquatic environment: A review. *Appl. Sci.* **2025**, *15*, 5182.
46. Badger, M.R. CO_2 concentrating mechanisms in cyanobacteria: Molecular components, their diversity and evolution. *J. Exp. Bot.* **2003**, *54*, 609–622.
47. Li, D.; Dong, H.; Cao, X.; et al. Enhancing photosynthetic CO_2 fixation by assembling metal-organic frameworks on *Chlorella pyrenoidosa*. *Nat. Commun.* **2023**, *14*, 5337.
48. Gao, W.; Guan, Y.; Li, Y.; et al. Treatment of nitrogen and phosphorus in wastewater by heterotrophic N- and P-starved microalgal cell. *Appl. Microbiol. Biotechnol.* **2023**, *107*, 1477–1490.
49. Perez-Garcia, O.; Escalante, F.M.E.; de-Bashan, L.E.; et al. Heterotrophic cultures of microalgae: Metabolism and potential products. *Water Res.* **2011**, *45*, 11–36.
50. Kumar, N.; Banerjee, C.; Chang, J.-S.; et al. Valorization of wastewater through microalgae as a prospect for generation of biofuel and high-value products. *J. Clean. Prod.* **2022**, *362*, 132114.
51. Hwang, J.-H.; Sadmani, A.; Lee, S.-J.; et al. An eco-friendly tool for the treatment of wastewaters for environmental safety. In *Bioremediation of Industrial Waste for Environmental Safety*; Bharagava, R., Saxena, G., Eds.; Springer: Singapore, 2020. https://doi.org/10.1007/978-981-13-3426-9_12.
52. Suresh Kumar, K.; Dahms, H.-U.; Won, E.-J.; et al. Microalgae—A promising tool for heavy metal remediation. *Ecotoxicol. Environ. Saf.* **2015**, *113*, 329–352.
53. Chakdar, H.; Thapa, S.; Srivastava, A.; et al. Genomic and proteomic insights into the heavy metal bioremediation by cyanobacteria. *J. Hazard. Mater.* **2022**, *424*, 127609.
54. Gaur, A.; Adholeya, A. Prospects of *arbuscular mycorrhizal* fungi in phytoremediation of heavy metal contaminated soils. *Curr. Sci.* **2004**, *86*, 528–534.
55. Sun, J.; Cheng, J.; Yang, Z.; et al. Microstructures and functional groups of *Nannochloropsis* sp. cells with arsenic adsorption and lipid accumulation. *Bioresour. Technol.* **2015**, *194*, 305–311.
56. Ananthi, V.; Raja, R.; Carvalho, I.S.; et al. A realistic scenario on microalgae based biodiesel production: Third generation biofuel. *Fuel* **2021**, *284*, 118965.
57. Mkpuma, V.O.; Moheimani, N.R.; Ennaceri, H. Effect of light intensity on *Chlorella* sp. biofilm growth on anaerobically digested food effluents (ADFE). *J. Environ. Manag.* **2024**, *371*, 123015.
58. Balbuena-Ortega, A.; Flores-Bahena, P.D.; Villa-Calderón, A.; et al. Impact of light spectrum on outdoors tubular

photobioreactors used for microalgae-based wastewater treatment. *J. Environ. Chem. Eng.* **2024**, *12*, 114884.
59. Khandelwal, A.; Chhabra, M.; Lens, P.N.L. Integration of third generation biofuels with bio-electrochemical systems: Current status and future perspective. *Front. Plant Sci.* **2023**, *14*. 1081108.
60. Wan Mahari, W.A.; Wan Razali, W.A.; Waiho, K.; et al. Light-emitting diodes (LEDs) for culturing microalgae and cyanobacteria. *Chem. Eng. J.* **2024**, *485*, 149619.
61. Yin, S.; Jin, W.; Xi, T.; et al. Factors affect the oxygen production of *Chlorella pyrenoidosa* in a bacterial-algal symbiotic system: Light intensity, temperature, pH and static magnetic field. *Process Saf. Environ. Prot.* **2024**, *184*, 492–501.
62. Sachdeva, N.; Gupta, R.P.; Mathur, A.S.; et al. Enhanced lipid production in thermo-tolerant mutants of *Chlorella pyrenoidosa* NCIM 2738. *Bioresour. Technol.* **2016**, *221*, 576–587.
63. Zhou, W.; Wang, Z.; Xu, J.; et al. Cultivation of microalgae *Chlorella zofingiensis* on municipal wastewater and biogas slurry towards bioenergy. *J. Biosci. Bioeng.* **2018**, *126*, 644–648.
64. Abdur Razzak, S.; Bahar, K.; Islam, K.M.O.; et al. Microalgae cultivation in photobioreactors: Sustainable solutions for a greener future. *Green Chem. Eng.* **2024**, *5*, 418–439.
65. Rosli, S.S.; Amalina Kadir, W.N.; Wong, C.Y.; et al. Insight review of attached microalgae growth focusing on support material packed in photobioreactor for sustainable biodiesel production and wastewater bioremediation. *Renew. Sustain. Energy Rev.* **2020**, *134*, 110306.
66. Sousa, S.A.; Machado, C.A.; Esteves, A.F.; et al. Microalgae-based wastewater remediation: Linking N:P ratio and nitrogen sources to treatment performance by *Chlorella vulgaris* and biomass valorisation. *Chem. Eng. J.* **2025**, *518*, 164701.
67. Longo, S.; d'Antoni, B.M.; Bongards, M.; et al. Monitoring and diagnosis of energy consumption in wastewater treatment plants. A state of the art and proposals for improvement. *Appl. Energy* **2016**, *179*, 1251–1268.
68. Sharma, A.; Chhabra, M. Performance evaluation of a photosynthetic microbial fuel cell (PMFC) using *Chlamydomonas reinhardtii* at cathode. *Bioresour. Technol.* **2021**, *338*, 125499.
69. Kakarla, R.; Kim, J.R.; Jeon, B.-H.; et al. Enhanced performance of an air-cathode microbial fuel cell with oxygen supply from an externally connected algal bioreactor. *Bioresour. Technol.* **2015**, *195*, 210–216.
70. Ullah, Z.; Sheikh, Z.; Zaman, W.Q.; et al. Performance comparison of a photosynthetic and mechanically aerated microbial fuel cell for wastewater treatment and bioenergy generation using different anolytes. *J. Water Process Eng.* **2023**, *56*, 104358.
71. Yahampath Arachchige Don, C.D.Y.; Babel, S. Comparing the performance of microbial fuel cell with mechanical aeration and photosynthetic aeration in the cathode chamber. *Int. J. Hydrogen Energy* **2021**, *46*, 16751–16761.
72. Kakarla, R.; Min, B. Photoautotrophic microalgae *Scenedesmus obliquus* attached on a cathode as oxygen producers for microbial fuel cell (MFC) operation. *Int. J. Hydrogen Energy* **2014**, *39*, 10275–10283.
73. Bazdar, E.; Roshandel, R.; Yaghmaei, S.; et al. The effect of different light intensities and light/dark regimes on the performance of photosynthetic microalgae microbial fuel cell. *Bioresour. Technol.* **2018**, *261*, 350–360.
74. Jang, J.K.; Kan, J.; Bretschger, O.; et al. Electricity generation by microbial fuel cell using microorganisms as catalyst in cathode. *J. Microbiol. Biotechnol.* **2013**, *23*, 1765–1773.
75. Noori, M.T.; Ghangrekar, M.M.; Mukherjee, C.K.; et al. Biofouling effects on the performance of microbial fuel cells and recent advances in biotechnological and chemical strategies for mitigation. *Biotechnol. Adv.* **2019**, *37*, 107420.
76. Li, J.; Chen, Z. Revitalizing microbial fuel cells: A comprehensive review on the transformative role of iron-based materials in electrode design and catalyst development. *Chem. Eng. J.* **2024**, *489*, 151323.
77. Qiu, S.; Guo, Z.; Naz, F.; et al. An overview in the development of cathode materials for the improvement in power generation of microbial fuel cells. *Bioelectrochemistry* **2021**, *141*, 107834.
78. Dange, P.; Savla, N.; Pandit, S.; et al. A comprehensive review on oxygen reduction reaction in microbial fuel cells. *JRM* **2021**, *10*, 665–697.
79. Sun, Y.; Li, H.; Guo, S.; et al. Metal-based cathode catalysts for electrocatalytic ORR in microbial fuel cells: A review. *Chin. Chem. Lett.* **2024**, *35*, 109418.
80. Liu, T.; Rao, L.; Yuan, Y.; et al. Bioelectricity generation in a microbial fuel cell with a self-sustainable photocathode. *Sci. World J.* **2015**, *2015*, 864568.
81. Zhao, C.-X.; Liu, J.-N.; Wang, J.; et al. Recent advances of noble-metal-free bifunctional oxygen reduction and evolution electrocatalysts. *Chem. Soc. Rev.* **2021**, *50*, 7745–7778.
82. Zhao, K.; Shu, Y.; Li, F.; et al. Bimetallic catalysts as electrocatalytic cathode materials for the oxygen reduction reaction in microbial fuel cell: A review. *Green Energy Environ.* **2023**, *8*, 1043–1070.
83. Wang, H.; Wei, L.; Yang, C.; et al. A pyridine-Fe gel with an ultralow-loading Pt derivative as ORR catalyst in microbial fuel cells with long-term stability and high output voltage. *Bioelectrochemistry* **2020**, *131*, 107370.
84. Li, M.; Zhou, J.; Bi, Y.-G.; et al. Transition metals (Co, Mn, Cu) based composites as catalyst in microbial fuel cells application: The effect of catalyst composition. *Chem. Eng. J.* **2020**, *383*, 123152.

85. Kodali, M.; Santoro, C.; Serov, A.; et al. P. Air breathing cathodes for microbial fuel cell using Mn-, Fe-, Co- and Ni-containing platinum group metal-free catalysts. *Electrochim. Acta* **2017**, *231*, 115–124.
86. Yang, Y.-W.; Li, M.-J.; Tao, W.-Q.; et al. Study of carbon dioxide sequestration and electricity generation by a new hybrid bioenergy system with the novelty catalyst. *Appl. Therm. Eng.* **2021**, *197*, 117366.
87. Abazarian, E.; Gheshlaghi, R.; Mahdavi, M.A. Impact of light/dark cycle on electrical and electrochemical characteristics of algal cathode sediment microbial fuel cells. *J. Power Sources* **2020**, *475*, 228686.
88. Zhang, Y.; He, Q.; Xia, L.; et al. Algae cathode microbial fuel cells for cadmium removal with simultaneous electricity production using nickel foam/graphene electrode. *Biochem. Eng. J.* **2018**, *138*, 179–187.
89. Dumas, C.; Mollica, A.; Féron, D.; et al. Marine microbial fuel cell: Use of stainless steel electrodes as anode and cathode materials. *Electrochim. Acta* **2007**, *53*, 468–473.
90. Neethu, B.; Ihjas, K.; Chakraborty, I.; et al. Nickel adsorbed algae biochar based oxygen reduction reaction catalyst. *Bioelectrochemistry* **2024**, *159*, 108747.
91. Elmaadawy, K.; Liu, B.; Hassan, G.; et al. Microalgae-assisted fixed-film activated sludge MFC for landfill leachate treatment and energy recovery. *Process Saf. Environ. Prot.* **2022**, *160*, 221–231.
92. Wu, X.; Song, T.; Zhu, X.; et al. Construction and operation of microbial fuel cell with *Chlorella Vulgaris* biocathode for electricity generation. *Appl. Biochem. Biotechnol.* **2013**, *171*, 2082–2092.
93. Altın, N.; Uyar, B. Increasing power generation and energy efficiency with modified anodes in algae-supported microbial fuel cells. *Biomass Conv. Bioref.* **2025**, *15*, 17203–17215.
94. Ling, J.; Xu, Y.; Lu, C.; et al. Enhancing stability of microalgae biocathode by a partially submerged carbon cloth electrode for bioenergy production from wastewater. *Energies* **2019**, *12*, 3229.
95. Xin, S.; Shen, J.; Liu, G.; et al. High electricity generation and COD removal from cattle wastewater in microbial fuel cells with 3D air cathode employed non-precious Cu_2O/reduced graphene oxide as cathode catalyst. *Energy* **2020**, *196*, 117123.
96. Wang, Y.; Zhong, K.; Li, H.; et al. Bimetallic hybrids modified with carbon nanotubes as cathode catalysts for microbial fuel cell: Effective oxygen reduction catalysis and inhibition of biofilm formation. *J. Power Sources* **2021**, *485*, 229273.
97. Du, Y.; Ma, F.-X.; Xu, C.-Y.; et al. Nitrogen-doped carbon nanotubes/reduced graphene oxide nanosheet hybrids towards enhanced cathodic oxygen reduction and power generation of microbial fuel cells. *Nano Energy* **2019**, *61*, 533–539.
98. Parsa, S.M.; Chen, Z.; Feng, S.; et al. Metal-free nitrogen-doped carbon-based electrocatalysts for oxygen reduction reaction in microbial fuel cells: Advances, challenges, and future directions. *Nano Energy* **2025**, *134*, 110537.
99. Guo, B.; Jiang, Q.; Mao, Z.; et al. B–F dual-doped carbon nanotubes for multi-site and high-rate two-electron oxygen reduction reaction electrocatalysis. *Carbon* **2024**, *222*, 118997.
100. Lv, Q.; Si, W.; He, J.; Sun, L.; et al. Selectively nitrogen-doped carbon materials as superior metal-free catalysts for oxygen reduction. *Nat. Commun.* **2018**, *9*, 3376.
101. Qin, L.; Liu, Y.; Qin, Y.; et al. Gd-Co nanosheet arrays coated on N-doped carbon spheres as cathode catalyst in photosynthetic microalgae microbial fuel cells. *Sci. Total Environ.* **2022**, *849*, 157711.
102. Yin, S.-H.; Yang, J.; Han, Y.; et al. Construction of highly active metal-containing nanoparticles and FeCo-N_4 composite sites for the acidic oxygen reduction reaction. *Angew. Chem. Int. Ed.* **2020**, *59*, 21976–21979.
103. Zhang, S.; Zhang, S.; Liu, H.; et al. Fe-N-C-based cathode catalyst enhances redox reaction performance of microbial fuel cells: Azo dyes degradation accompanied by electricity generation. *J. Environ. Chem. Eng.* **2023**, *11*, 109264.
104. Cheng, S.; Wu, J. Air-cathode preparation with activated carbon as catalyst, PTFE as binder and nickel foam as current collector for microbial fuel cells. *Bioelectrochemistry* **2013**, *92*, 22–26.
105. Li, X.; Hu, B.; Suib, S.; et al. Manganese dioxide as a new cathode catalyst in microbial fuel cells. *J. Power Sources* **2010**, *195*, 2586–2591.
106. Zhang, X.; Lin, Z.; Liang, B.; et al. Highly efficient improvement of power generation and novel porous iron-nitrogen-doped carbon nanosphere. *J. Power Sources* **2021**, *498*, 229883.
107. Ortiz-Martínez, V.M.; Salar-García, M.J.; Touati, K.; et al. Assessment of spinel-type mixed valence Cu/Co and Ni/Co-based oxides for power production in single-chamber microbial fuel cells. *Energy* **2016**, *113*, 1241–1249.
108. Wang, J.; Zhang, P.; Yang, B.; et al. Cu/TiO_2 Nanoparticles: Enhancing microbial fuel cell performance as photocathode catalysts. *Bioresour. Technol.* **2025**, *430*, 132586.
109. Yan, Y.; Hou, Y.; Yu, Z.; et al. Bimetallic organic framework-derived, oxygen-defect-rich $FexCo_{3-x}S_4$/$Fe_yCo_{9-y}S_8$ heterostructure microsphere as a highly efficient and robust cathodic catalyst in the microbial fuel cell. *J. Power Sources* **2020**, *472*, 228582.
110. Wang, H.; Wei, L.; Shen, J. Iron-gelatin aerogel derivative as high-performance oxygen reduction reaction electrocatalysts in microbial fuel cells. *Int. J. Hydrogen Energy* **2022**, *47*, 17982–17991.
111. Yang, W.; Wang, X.; Rossi, R.; et al. Low-cost Fe–N–C catalyst derived from Fe (III)-chitosan hydrogel to enhance power production in microbial fuel cells. *Chem. Eng. J.* **2020**, *380*, 122522.

112. Song, Y.; Zhen, F.; Qi, Y.; et al. One-step annealing in situ synthesis of low tortuosity corn straw cellulose biochar/Fe_3C: Application for cathode catalyst in microbial fuel cell. *Int. J. Biol. Macromol.* **2025**, *289*, 138750.
113. Peera, S.G.; Maiyalagan, T.; Liu, C.; et al. A review on carbon and non-precious metal based cathode catalysts in microbial fuel cells. *Int. J. Hydrogen Energy* **2021**, *46*, 3056–3089.
114. Sun, Y.; Duan, Y.; Hao, L.; et al. Cornstalk-derived nitrogen-doped partly graphitized carbon as efficient metal-free catalyst for oxygen reduction reaction in microbial fuel cells. *ACS Appl. Mater. Interfaces* **2016**, *8*, 25923–25932.
115. Ma, Y.; You, S.; Jing, B.; et al. Biomass pectin-derived N, S-enriched carbon with hierarchical porous structure as a metal-free catalyst for enhancing bio-electricity generation. *Int. J. Hydrogen Energy* **2019**, *44*, 16624–16638.
116. Liang, B.; Li, K.; Liu, Y.; et al. Nitrogen and phosphorus dual-doped carbon derived from chitosan: An excellent cathode catalyst in microbial fuel cell. *Chem. Eng. J.* **2019**, *358*, 1002–1011.
117. Chang, H.-C.; Gustave, W.; Yuan, Z.-F.; et al. One-step fabrication of binder-free air cathode for microbial fuel cells by using balsa wood biochar. *Environ. Technol. Innov.* **2020**, *18*, 100615.
118. Chakraborty, I.; Sathe, S.M.; Dubey, B.K.; et al. Waste-derived biochar: Applications and future perspective in microbial fuel cells. *Bioresour. Technol.* **2020**, *312*, 123587.
119. Zhao, S.; Liu, S.; Sumpradit, T.; et al. Magnetic nanoparticles doped biochar cathode in a two-chamber microbial fuel cell for the adsorption-reduction of hexavalent chromium. *Int. J. Hydrogen Energy* **2024**, *63*, 163–172.
120. Zhang, K.; Zhao, Z.; Luo, H.; et al. Enhanced the treatment of antibiotic wastewater and antibiotic resistance genes control by Fe^0-catalyzed microalgal MFCs in continuous flow mode. *J. Water Process Eng.* **2023**, *53*, 103701.
121. Sun, J.; Li, N.; Yang, P.; et al. Simultaneous antibiotic degradation, simultaneous antibiotic degradation, nitrogen removal and power generation in a microalgae-bacteria powered biofuel cell designed for aquaculture wastewater treatment and energy recovery. *Int. J. Hydrogen Energy* **2020**, *45*, 10871–10881.
122. Wang, Y.; Lin, Z.; Su, X.; et al. Cost-effective domestic wastewater treatment and bioenergy recovery in an immobilized microalgal-based photoautotrophic microbial fuel cell (PMFC). *Chem. Eng. J.* **2019**, *372*, 956–965.
123. Elmaadawy, K.; Hu, J.; Guo, S.; et al. Enhanced treatment of landfill leachate with cathodic algal biofilm and oxygen-consuming unit in a hybrid microbial fuel cell system. *Bioresour. Technol.* **2020**, *310*, 123420.
124. Jiang, Q.; Song, X.; Liu, J.; et al. Enhanced nutrients enrichment and removal from eutrophic water using a self-sustaining in situ photomicrobial nutrients recovery cell (PNRC). *Water Res.* **2019**, *167*, 115097.
125. Logroño, W.; Pérez, M.; Urquizo, G.; et al. Single chamber microbial fuel cell (SCMFC) with a cathodic microalgal biofilm: A preliminary assessment of the generation of bioelectricity and biodegradation of real dye textile wastewater. *Chemosphere* **2017**, *176*, 378–388.
126. Zieliński, M.; Rusanowska, P.; Dudek, M.; et al. Efficiency of photosynthetic microbial fuel cells (pMFC) depending on the type of microorganisms inhabiting the cathode chamber. *Energies* **2024**, *17*, 2296.
127. Deka, R.; Shreya, S.; Mourya, M.; et al. A techno-economic approach for eliminating dye pollutants from industrial effluent employing microalgae through microbial fuel cells: Barriers and perspectives. *Environ. Res.* **2022**, *212*, 113454.
128. Iniesta-López, E.; Fernández, A.H.; Gómez, J.M.; et al. Transforming waste management: Converting pig slurry into clean energy and biomass through integrated MFC-microalgae systems. *J. Water Process Eng.* **2025**, *69*, 106815.
129. Bora, A.; Gurusamy, S.; Veleeswaran, A.; et al. Simultaneous biodiesel and bioelectricity generation utilizing dairy and rice mill wastewater by freshwater microalgal isolate: An integrated energy-efficient approach. *Process Saf. Environ. Prot.* **2024**, *190*, 149–161.
130. Yang, Z.; Nie, C.; Hou, Q.; et al. Coupling a photosynthetic microbial fuel cell (PMFC) with photobioreactors (PBRs) for pollutant removal and bioenergy recovery from anaerobically digested effluent. *Chem. Eng. J.* **2019**, *359*, 402–408.
131. Pengadeth, D.; Prakash Naik, S.; Sasi, A.; et al. Revisiting the role of algal biocathodes in microbial fuel cells for bioremediation and value-addition. *Chem. Eng. J.* **2024**, *496*, 154144.
132. Yang, Z.; Pei, H.; Hou, Q.; et al. Algal biofilm-assisted microbial fuel cell to enhance domestic wastewater treatment: Nutrient, organics removal and bioenergy production. *Chem. Eng. J.* **2018**, *332*, 277–285.
133. Yang, Z.; Li, J.; Chen, F.; et al. Bioelectrochemical process for simultaneous removal of copper, ammonium and organic matter using an algae-assisted triple-chamber microbial fuel cell. *Sci. Total Environ.* **2021**, *798*, 149327.
134. Verma, M.; Singh, V.; Mishra, V. Bioelectricity generation by using cellulosic waste and spent engine oil in a concentric photobioreactor-microbial fuel cell. *J. Environ. Chem. Eng.* **2023**, *11*, 110566.
135. Nguyen, H.T.H.; Min, B. Leachate treatment and electricity generation using an algae-cathode microbial fuel cell with continuous flow through the chambers in series. *Sci. Total Environ.* **2020**, *723*, 138054.
136. Pannell, T.C.; Goud, R.K.; Schell, D.J.; et al. Effect of fed-batch *vs.* continuous mode of operation on microbial fuel cell performance treating biorefinery wastewater. *Biochem. Eng. J.* **2016**, *116*, 85–94.
137. Sharma, M.; Jalalah, M.; Alsareii, S.A.; et al. Microalgal cycling in the cathode of microbial fuel cells (MFCs) induced oxygen reduction reaction (ORR) and electricity: A biocatalytic process for clean energy. *Chem. Eng. J.* **2024**, *479*, 147431.

138. Qin, L.; Qin, Y.; Cui, N.; et al. Photosynthetic microalgae microbial fuel cells for bioelectricity generation and microalgae lipid recovery using Gd-Co@N-CSs/NF as cathode. *Chem. Eng. J.* **2024**, *490*, 151647.
139. You, J.; Guo, Y.; Guo, R.; et al. A review of visible light-active photocatalysts for water disinfection: Features and prospects. *Chem. Eng. J.* **2019**, *373*, 624–641.
140. Hao, A.; Ning, X.; Liu, X.; et al. Phosphorus heteroatom doped BiOCl as efficient catalyst for photo-piezocatalytic degradation of organic pollutant and unveiling the mechanism: Experiment and DFT calculation. *Chem. Eng. J.* **2024**, *499*, 155823.
141. Zhu, X.; Zhang, Y.; Wang, Y.; et al. Oxygen-deficient WO_3 for stable visible-light photocatalytic degradation of acetaldehyde within a wide humidity range. *Chem. Eng. J.* **2024**, *491*, 152193.
142. Nosaka, Y.; Nosaka, A.Y. Generation and detection of reactive oxygen species in photocatalysis. *Chem. Rev.* **2017**, *117*, 11302–11336.
143. Lan, Y.; Li, Z.; Li, D.; et al. Visible-light responsive Z-scheme Bi@β-Bi_2O_3/g-C_3N_4 heterojunction for efficient photocatalytic degradation of 2,3-dihydroxynaphthalene. *Chem. Eng. J.* **2020**, *392*, 123686.
144. Yuan, C.; Tian, N.; Gao, L.; et al. Efficient dual functional hydrogen production synergistic degradation of organic pollutants by hydroxyl and cyano group modified crystalline g-C_3N_4 under visible light. *Chem. Eng. J.* **2025**, *503*, 158645.
145. Shi, K.; Wang, J.; Yin, L.; et al. Efficient synergistic degradation of tetracycline hydrochloride by protonated g-C_3N_4 and *Chlorella pyrenoidosa*: Kinetics and mechanism. *Chem. Eng. J.* **2023**, *462*, 142331.
146. Li, Z.; Chen, G.; Cheng, P.; et al. Phototactic photocatalysis enabled by functionalizing active microorganisms with photocatalyst. *Adv. Sustain. Syst.* **2024**, *8*, 2300302.
147. Wang, L.; Zhang, C.; Gao, F.; et al. Algae decorated TiO_2/Ag hybrid nanofiber membrane with enhanced photocatalytic activity for Cr(VI) removal under visible light. *Chem. Eng. J.* **2017**, *314*, 622–630.
148. Lu, Z.; Xu, Y.; Peng, L.; et al. A two-stage degradation coupling photocatalysis to microalgae enhances the mineralization of enrofloxacin. *Chemosphere* **2022**, *293*, 133523.
149. Gao, W.; Pan, X.; Wu, J.; et al. Synergistic degradation mechanism of roxithromycin by the combination of TiO_2/graphene oxide/polypropylene fiber photocatalytic network and microalgae. *Chem. Eng. J.* **2025**, *519*, 165218.
150. Zhang, D.; Yang, H.; Guo, X.; et al. Visible-light-driven synergistic photocatalysis-microbial metabolism by *Chlorella ellipsoidea*@TiO_2-Ag-AgCl nano-biohybrid: Enhanced *o*-cresol biodegradation and mechanistic insights. *J. Hazard. Mater.* **2025**, *495*, 138771.
151. Xiao, C.; Yuan, J.; Li, L.; et al. Photocatalytic synergistic biofilms enhance tetracycline degradation and conversion. *Environ. Sci. Ecotechnol.* **2023**, *14*, 100234.
152. Lee H, Hyun J. Biophotovoltaic living hydrogel of an ion-crosslinked carboxymethylated cellulose nanofiber/alginate. *Carbohydr. Polym*. **2023**, *321*, 121299.
153. Liu, S.; Ma, L.; Liu, Y.; et al. Impact of photocatalysis, carriers and environmental factors on microorganisms in the intimate coupling of photocatalysis and biodegradation system: A review. *J. Environ. Chem. Eng.* **2024**, *12*, 113136.
154. Singh, R.; Sinha, A. A critical review of recent advancements in the photocatalysis process, mechanism, and degradation pathways for the removal of phthalates from the contaminated water matrix. *J. Environ. Manag.* **2025**, *377*, 124663.
155. Zhong, N.; Yuan, J.; Luo, Y.; et al. Intimately coupling photocatalysis with phenolics biodegradation and photosynthesis. *Chem. Eng. J.* **2021**, *425*, 130666.
156. Ding, X.; Yu, Q.; Ren, H.; et al. Degradation of conjugated estrogen in visible light-driven intimately coupled photocatalysis and biodegradation system. *Bioresour. Technol.* **2024**, *406*, 131045.
157. Zhang, H.; Yu, Y.; Li, Y.; et al. A novel BC/g-C_3N_4 porous hydrogel carrier used in intimately coupled photocatalysis and biodegradation system for efficient removal of tetracycline hydrochloride in water. *Chemosphere* **2023**, *317*, 137888.
158. Dong, Y.; Xu, D.; Zhang, J.; et al. Enhanced antibiotic wastewater degradation by intimately coupled B-Bi_3O_4Cl photocatalysis and biodegradation reactor: Elucidating degradation principle systematically. *J. Hazard. Mater.* **2023**, *445*, 130364.
159. Wang, J.; Xiong, J.; Feng, Q.; et al. Intimately coupled photocatalysis and functional bacterial system enhance degradation of 1,2,3- and 1,3,5-trichlorobenzene. *J. Environ. Manag.* **2022**, *318*, 115595.
160. Zhu, C.; Huang, Y.; Ding, Z.; et al. Development and mechanistic insights of a photocatalytic-algae-bacteria degradation coupling system for treating toxic coking wastewater. *J. Environ. Sci.* **2025**, *157*, 296–308.
161. Wen, D.; Li, G.; Xing, R.; et al. 2,4-DNT removal in intimately coupled photobiocatalysis: The roles of adsorption, photolysis, photocatalysis, and biotransformation. *Appl. Microbiol. Biotechnol.* **2012**, *95*, 263–272.
162. Cai, H.; Sun, L.; Wang, Y.; et al. Unprecedented efficient degradation of phenanthrene in water by intimately coupling novel ternary composite Mn_3O_4/MnO_2-Ag_3PO_4 and functional bacteria under visible light irradiation. *Chem. Eng. J.* **2019**, *369*, 1078–1092.
163. Peng, L.; Long, Q.; Liang, C.; et al. Efficient degradation of sulfamonomethoxine in wastewater using a novel intimately coupled photocatalysis and biodegradation system prepared with the calcium alginate hydrogel. *Biochem. Eng. J.* **2025**,

219, 109731.
164. Guo, J.; Guo, X.; Yang, H.; et al. Construction of Bio-TiO_2/Algae complex and synergetic mechanism of the acceleration of phenol biodegradation. *Materials* **2023**, *16*, 3882.
165. Xiong, J.-Q.; Kurade, M.B.; Jeon, B.-H. Can microalgae remove pharmaceutical contaminants from water? *Trends Biotechnol.* **2018**, *36*, 30–44.
166. Guo, J.; Song, G.; Zhou, M. Highly dispersed FeN-CNTs heterogeneous electro-Fenton catalyst for carbamazepine removal with low Fe leaching at wide pH. *Chem. Eng. J.* **2023**, *474*, 145681.
167. Deng, Z.; Gong, Z.; Gong, M.; et al. Defect engineering on commercial carbon for economical H_2O_2 electrosynthesis under industrial-relevant conditions. *Adv. Funct. Mater.* **2025**, e12847.
168. Xue, S.; Li, X.; Sun, Y.; et al. Hydrogen radical enabling industrial-level oxygen electroreduction to hydrogen peroxide. *Angew. Chem. Int. Ed.* **2025**, *64*, e202420063.
169. Deng, F.; Olvera-Vargas, H.; Zhou, M.; et al. Critical review on the mechanisms of Fe^{2+} regeneration in the electro-Fenton process: Fundamentals and boosting strategies. *Chem. Rev.* **2023**, *123*, 4635–4662.
170. Monteil, H.; Péchaud, Y.; Oturan, N.; et al. A review on efficiency and cost effectiveness of electro- and bio-electro-Fenton processes: Application to the treatment of pharmaceutical pollutants in water. *Chem. Eng. J.* **2019**, *376*, 119577.
171. Nidheesh, P.V.; Ganiyu, S.O.; Martínez-Huitle, C.A.; et al. Recent advances in electro-Fenton process and its emerging applications. *Crit. Rev. Environ. Sci. Technol.* **2023**, *53*, 887–913.
172. Jiménez-Bambague, E.M.; Villarreal-Arias, D.S.; Ramírez-Vanegas, O.D.; et al. Removal of pharmaceutical compounds from real urban wastewater by a continuous bio-electrochemical process at pilot scale. *J. Environ. Chem. Eng.* **2023**, *11*, 110130.
173. Mousset, E.; Trellu, C.; Olvera-Vargas, H.; et al. A. Electrochemical technologies coupled with biological treatments. *Curr. Opin. Electrochem.* **2021**, *26*, 100668.
174. Zhu, M.; Liu, X.; Liu, L.; et al. MFC based in situ electrocatalytic persulfate activation for degradation of 2,4-dichlorophenol: Process and mechanism. *J. Environ. Chem. Eng.* **2022**, *10*, 108803.
175. Xie, Z.; Yang, C.; Yu, X.-Y.; et al. Direct extracellular electron transfer for high electricity production by a new type of marine microalgae *Nannochloropsis* sp. HDY2. *Chem. Eng. J.* **2024**, *481*, 148636.
176. Deng, Z.; Ma, Y.; Zhu, J.; et al. In situ activation of peroxymonosulfate with bioelectricity for sulfamethoxazole sustainable removal. *Environ. Res.* **2024**, *257*, 119294.
177. Miranda, D.E.E.; Paricahua, R.M.A.; Quispe, E.N.G.; et al. Sequential treatment of tannery wastewater using microalgae and microwave-prepared anodes. *Chemosphere* **2025**, *386*, 144619.
178. Chen, Y.; Lv, Z.; Xu, J.; et al. Stainless steel mesh coated with MnO_2/carbon nanotube and polymethylphenyl siloxane as low-cost and high-performance microbial fuel cell cathode materials. *J. Power Sources* **2012**, *201*, 136–141.
179. Bhaduri, S.; Behera, M. From single-chamber to multi-anodic microbial fuel cells: A review. *J. Environ. Manag.* **2024**, *355*, 120465.
180. Sayed, E.T.; Rezk, H.; Abdelkareem, M.A.; et al. Artificial neural network based modelling and optimization of microalgae microbial fuel cell. *Int. J. Hydrogen Energy* **2024**, *52*, 1015–1025.
181. Ren, Z.; Li, H.; Sun, P.; et al. Development and challenges of emerging biological technologies for algal-bacterial symbiosis systems: A review. *Bioresour. Technol.* **2024**, *413*, 131459.
182. He, Q.; Zhang, Q.; Li, M.; et al. Harnessing diurnal dynamics: Understanding the influence of light–dark cycle on algal-bacterial symbiotic system under aniline stress. *Bioresour. Technol.* **2025**, *416*, 131796.
183. Ewusi-Mensah, D.; Huang, J.; Chaparro, L.K.; et al. Algae-assisted microbial desalination cell: Analysis of cathode performance and desalination efficiency assessment. *Processes* **2021**, *9*, 2011.
184. Qing, S.; Lu, X.; Jiang, Y.; et al. ZIF-8 confined carbon dots/bilirubin oxidase on microalgal cells to boost oxygen reduction reaction in photo-biocatalytic fuel cells for pollutants removal. *Chin. Chem. Lett.* **2024**, 110576. https://doi.org/10.1016/j.cclet.2024.110576.
185. Wang, X.; Hu, J.; Chen, Q.; et al. Synergic degradation of 2,4,6-trichlorophenol in microbial fuel cells with intimately coupled photocatalytic-electrogenic anode. *Water Res.* **2019**, *156*, 125–135.
186. Xu, Z.; Chen, S.; Guo, S.; et al. New insights in light-assisted microbial fuel cells for wastewater treatment and power generation: A win-win cooperation. *J. Power Sources* **2021**, *501*, 230000.
187. Si, Q.; Feng, X.; Teng, Y.; et al. C Constructing effective and low-toxic removal of combined contaminants by intimately coupled Z-scheme heterojunction photocatalysis and biodegradation system. *Appl. Catal. B Environ.* **2025**, *365*, 124909.
188. Ranade, A.K.; Yamaguchi, A.; Miyauchi, M.; et al. Interface dependent electron shunting in graphene-integrated intimately coupled photocatalytic biodegradation. *Water Res.* **2025**, *273*, 123064.
189. Mishra, A.; Medhi, K.; Malaviya, P.; et al. Omics approaches for microalgal applications: Prospects and challenges. *Bioresour. Technol.* **2019**, *291*, 121890.
190. Li, X.; Jia, X.; Zhang, C.; et al. A comprehensive overview of advances in heterogeneous electro-Fenton processes for

effective water treatment. *Sep. Purif. Technol.* **2025**, *361*, 131470.
191. Qin, X.; Cao, P.; Quan, X.; et al. Highly efficient hydroxyl radicals production boosted by the atomically dispersed Fe and Co sites for heterogeneous electro-Fenton oxidation. *Environ. Sci. Technol.* **2023**, *57*, 2907–2917.
192. Su, P.; Fu, W.; Hu, Z.; et al. Insights into transition metal encapsulated N-doped CNTs cathode for self-sufficient electrocatalytic degradation. *Appl. Catal. B Environ.* **2022**, *313*, 121457.
193. Cao, S.; Teng, F.; Lv, J.; et al. Performance of an immobilized microalgae-based process for wastewater treatment and biomass production: Nutrients removal, lipid induction, microalgae harvesting and dewatering. *Bioresour. Technol.* **2022**, *356*, 127298.
194. Liu, Y.; Zhang, G.; Li, Y.; et al. Enhancing immobilized *Chlorella vulgaris* growth with novel buoyant barium alginate bubble beads. *Bioresour. Technol.* **2024**, *406*, 130996.
195. Chen, Z.; McCuskey, S.R.; Zhang, W.; et al. Three-dimensional conductive conjugated polyelectrolyte gels facilitate interfacial electron transfer for improved biophotovoltaic performance. *Nat. Commun.* **2025**, *16*, 5955.